



NTNU – Trondheim
Norwegian University of
Science and Technology

Fatigue Assessment of Components Subjected to Non-Proportional Stress Histories

Øyvind Aleksander Bruun

Master of Science in Mechanical Engineering

Submission date: December 2013

Supervisor: Gunnar Härkegård, IPM

Co-supervisor: Bjørn Haugen, IPM

Norwegian University of Science and Technology
Department of Engineering Design and Materials

THE NORWEGIAN UNIVERSITY
OF SCIENCE AND TECHNOLOGY
DEPARTMENT OF ENGINEERING DESIGN
AND MATERIALS

**MASTER THESIS AUTUMN 2013
FOR
STUD.TECHN. ØYVIND A. BRUUN**

**FATIGUE ASSESSMENT OF COMPONENTS SUBJECTED TO NON-
PROPORTIONAL STRESS HISTORIES**

Utmattingsvurdering av komponenter utsatte for ikke-proporsjonale spenningshistorier

Traditional *S-N* based fatigue assessment criteria focus on uniaxial, constant amplitude loading. These criteria may be extended to multiaxial, variable-amplitude stress histories under *proportional* loading by introducing an ‘equivalent’ stress, such as the maximum principal stress amplitude or the von Mises stress amplitude (Sines, Crossland), together with suitable cycle-counting rules. The complexity of fatigue assessment is considerably increased, if *non-proportional* stress histories are considered. Although several ‘critical-plane’ theories (Findley, Dang Van, Matake, McDiarmid) have been proposed and implemented in FEA post-processors for fatigue assessment of components under arbitrary multiaxial stress histories, these theories are still not well established in engineering design.

When it comes to fatigue assessment based on fatigue-crack growth (FCG) in components under arbitrary multiaxial stress histories, the situation is even more unsatisfactory. Again most criteria and analytical tools assume uniaxial, constant amplitude loading. For multiaxial variable amplitude stress histories under proportional loading, crack growth is often assumed to be controlled by the maximum principal stress cycle.

In a preceding project work (Bruun, 2013), a critical assessment was carried out of ‘normal-stress modified’ shear-stress based critical-plane models (due to Findley and Sines) and a maximum-principal-stress based critical-plane type model (due to Hempel-Morrow) for the fatigue limit of a thin-walled tube under non-proportional normal-stress and shear-stress histories.

The objective of this master assignment is to extend the project work to a broader set of models for the fatigue assessment of components subjected to non-proportional stress histories. The work should include *S-N* as well as FCG based criteria, applied to critical-load prediction for stress-histories *below* the fatigue limit and to fatigue-life prediction for stress-histories *above* the fatigue limit. In the latter case, suitable cycle-counting rules are to be discussed. Whenever possible, theoretical predictions should be compared with observations from fatigue testing.

The thesis should be written as a scientific report including

- the (signed) project assignment,
- a summary of the work (in English and Norwegian),
- a table of contents,
- the inducement and purpose of the assignment,
- a presentation, demonstration and critical assessment of methods,
- results, conclusions and recommendations, and
- literature references.

Figures and tables (including captions) should be largely self-explanatory. Figures and tables supporting the main report, but not immediately required, can be included in one or more appendices. Literature sources should be suitably referenced in the text, and references should be specified in a standardised manner, generally including author(s), book title and publisher or title (and volume) of journal and paper, year of publication, and relevant page numbers. All figures, tables and literature references (and appendices) should be explicitly referred to in the thesis.

The evaluation of the master thesis will emphasise its clarity and thoroughness. It is also important that the author gives an independent presentation of the topic using views and insights developed in the thesis work.

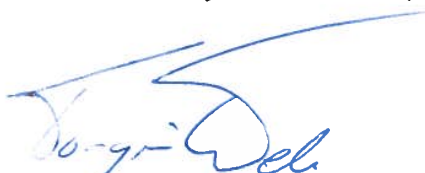
Three weeks after the start of the thesis work, an A3 sheet illustrating the work is to be handed in. A template for this presentation is available on the IPM website under the menu "Masteroppgave" (<http://www.ntnu.no/ipm/masteroppgave>). This sheet should be updated one week before submission of the thesis.

The thesis shall be submitted electronically via DAIM, NTNU's system for digital archiving and submission of master theses.

Contact persons:

At the department : Bjørn Haugen, Professor/Co-supervisor

From the industry : LINKftr (contact person to be named by August 2013)



Torgeir Welo
Head of Division

Gunnar Härkegård
Professor/Supervisor

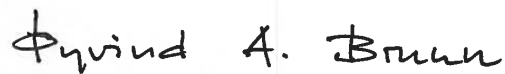


NTNU
Norges teknisk-
naturvitenskapelige universitet
Institutt for produktutvikling
og materialer

Preface

This Master's thesis, titled *Fatigue Assessment of Components Subjected to Non-Proportional Stress Histories*, was written as my final work in Mechanical Engineering at the Norwegian University of Science and Technology (NTNU). It serves as a direct continuation of an in-depth project work, completed in spring 2013. As a scientific thesis, this is the product of one intense year spent in the complex world of multiaxial fatigue. As my last assignment as a student at NTNU, it entails every bit of experience and knowledge I have gained throughout my years as a student.

There are several I would like to direct my utmost gratitude to. Special thanks go to my supervisor and professor Gunnar Härkegård. During interesting discussions, and through his powers of persuasion and commitment, I have now ventured deeper into the world of fatigue than I previously thought possible. I also wish to thank my family and girlfriend for all encouragement, patience and support.

A handwritten signature in black ink that reads "Øyvind A. Bruun". The signature is written in a cursive style with a vertical line through the middle of the text.

Øyvind A. Bruun

Trondheim, December 17th, 2013

Abstract

The fatigue assessment of components subjected to complex loading histories is a challenging topic. Several criteria intended for use under multiaxial stress-states and non-proportional loading have been proposed by many researchers throughout the years. This thesis is intended as a critical review of the fatigue assessment of both proportional and non-proportional stress histories.

A database consisting of 268 experimental tests for biaxial fatigue limits were collected from various sources. The compiled database spans 20 materials, ranging from carbon steels to cast irons. The data were evaluated using five multiaxial fatigue criteria and two separate assessment methods. The first assessment method is here described as the *proportional-method*, which is the assessment of relevant stress-values based on extreme values occurring throughout a cycle. The second method, here simply called the *ASME-method*, is heavily inspired by the ASME-criterion as stated by the ASME Boiler and Pressure Vessel code. The latter method determines the relevant stress values based on relative differences in stress components over time. In addition to the fatigue test data, a stress cycle provided from the industry is examined and discussed.

The lack of readily available fatigue test data for validating purposes is a serious concern that is discussed here. The database provided in the appendix is intended to partially remedy this, and serve as a starting point for future research. A comparison of predictions, both criteria- and methodology-wise is also provided. The results and findings are then critically discussed.

The research shows that the predictability of a fatigue criterion depends on both material and stress-state. For brittle materials such as the cast irons included in the assessment, the normal stress criterion provides excellent results. For carbon and low alloy steels, as well as the aluminium alloy 76S-T61, shear stress criteria such as Findley yield more accurate predictions. The ASME-method increases the complexity of the fatigue assessment, but is shown to have a positive effect on predictions for the Findley criterion.

Sammendrag

Utmattingsanalyse av komponenter utsatt for komplekse spenningshistorier er et utfordrende tema. Flere kriterier beregnet for bruk ved fleraksede spenningstilstander og ikke-proporsjonal belastning er gjennom årene blitt foreslått. Denne masteroppgaven har til hensikt å gi et kritisk innblikk i utmattingsanalysen av spenningshistorier av både proporsjonal og ikke-proporsjonal natur.

I den forbindelse ble det samlet en database bestående av totalt 268 eksperimentelt bestemte utmattingsgrenser for kombinerte belastninger. Utmattingsgrensene er fordelt på 20 ulike materialer og tilsammen 27 testserier. Disse ble så evaluert ved bruk av fem ulike utmattingskriterier og to forskjellige fremgangsmåter. Den ene fremgangsmåten er den klassiske, *proporsjonale* fremgangsmåten for å bestemme spenningsverdier som amplituder på. Denne metoden benytter seg av ekstremverdier som inntreffer gjennom hele spenningssyklusen sett over ett. Den andre metoden, baserer seg på ASME-kriteriet som gjengitt i ASME Boiler and Pressure Vessel Code. Sistnevnte metode beregner spenningsverdier basert på deres relative forskjeller over tid. I tillegg til utmattingsgrensene gjengitt i databasen, ble også en spenningssykel hentet fra industrien gjennomgått og diskutert.

Manglende tilgang på testdata er en kilde til bekymring, og blir grundig diskutert. I den anledning er utmattingsdataene samlet i databasen gjengitt som vedlegg, og slik er de enkelt tilgjengelig for videre bruk.

Resultatet av undersøkelsen indikerer at nøyaktigheten på prediksjonene fra et utmattingskriterium avhenger av både materiale og spenningstilstand. For sprø materialer slik som støpejern, gir normalspenningskriteriet uovertrufne resultater. For karbonstål og lavlegerte stål samt aluminiumslegeringen 76S-T61 gir skjærspenningskriterier som Findley de beste resultatene. For noen kriterier, da spesielt Findley-kriteriet, bidrar ASME-metoden til mer nøyaktige prediksjoner. I bruk bidrar ASME-metoden til at utmattingsanalysen generelt blir mer utfordrende.

Nomenclature

\hat{t}	critical point in time	[sec]
I_1	first stress invariant	[MPa]
\bar{X}	arithmetic mean value of random discrete variable	
a	support factor from FKM-Richtlinie	
b	support factor from FKM-Richtlinie	
f_{crit}	critical parameter (Findley)	
$f_{w,\sigma}$	constant used by FKM	
$f_{w,\tau}$	constant used by FKM	
k	Findley constant	
M	mean stress sensitivity	
m_p	mean value of predictions	
n	number of variables	
N_f	cycles to failure	
P	loading parameter	
R	relationship between max. and min. stress	
R_m	ultimate tensile strength	[MPa]
s	sample standard deviation	
s_p	sample standard deviation of predictions	
T	length of stress history	[sec]

t time [sec]

X_i discrete variable

Vectors and matrixes

\mathbf{I}_1 first stress invariant matrix

\mathbf{n} unit normal vector

\mathbf{S} cartesian stress tensor

\mathbf{x} placement in a body

Greek Symbols

α phase shift [deg]

β constant

$\hat{\phi}$ angle between x-axis and largest principal stress [°]

λ constant

ω angular frequency [rad/sec]

ϕ azimuth angle between x-axis and unit normal vector [°]

σ' modified stress according to the ASME criterion [MPa]

σ_h hydrostatic stress [MPa]

σ'_f fatigue strength coefficient [MPa]

Σ stress field for $P=1$

σ normal stress [MPa]

$\sigma_{1,2}$ principal stresses [MPa]

σ_A purely pulsating fatigue limit for tension/bending [MPa]

σ_W fatigue limit for fully reversed normal stress [MPa]

σ_{ar} equivalent fully reversed stress amplitude [MPa]

$\sigma_{eq,T}$ Tresca equivalent stress [MPa]

σ_{eq}	von Mises equivalent stress	[MPa]
τ	shear stress	[MPa]
τ_A	fatigue limit for purely pulsating shear stress	[MPa]
τ_W	fully reversed fatigue limit in shear	[MPa]
θ	polar angle	[°]
S'	difference between principal stresses (ASME criterion)	[MPa]

Subscripts

a	amplitude of given stress component
\max	maximum value of a given stress component
\min	minimum value of a given stress component
m	mean value of a given stress component
A, B	indication of case A or case B crack growth
ij	element of a given stress component in cartesian stress tensor

Contents

Preface	I
Abstract	II
Sammendrag	III
Nomenclature	IV
1. Introduction	1
1.1. Limitation of Investigation	2
1.2. Previous Research	3
2. Literature Review	5
2.1. Stress Analysis	5
2.1.1. Static Stress Analysis	5
2.1.2. Dynamic Stress Analysis	7
2.1.3. Special Case of Plane Stress	8
2.2. Uniaxial Fatigue Analysis	9
2.3. Multiaxial Fatigue Criteria	10
2.3.1. Normal Stress Criterion	11
2.3.2. Mises-Sines Criterion	11
2.3.3. Tresca-Sines Criterion	11
2.3.4. ASME-Criterion for Non-Proportional Loading	12
2.3.5. Findley Criterion	13
2.3.6. Other Fatigue Criteria	14
2.3.6.1. Crossland Criterion	14
2.3.6.2. McDiarmid Criterion	14
2.3.6.3. Mataka Criterion	15
2.4. Statistical Analysis	15
2.5. FKM-Richtlinie	15
3. Fatigue Test Database	17

4. Procedure	21
4.1. General Procedure for Fatigue Assessment	21
4.2. Normalizing of Stresses	22
4.3. Determination of Material Parameters and Constants	22
4.4. Modelling of Stress Histories	22
4.5. Proportional Method for Determination of Criteria	23
4.6. ASME Method for Determination of Criteria	23
4.7. Computational Algorithm	25
4.8. Failure Assessment Diagrams	27
4.8.1. Algorithm and Plotting	28
4.8.2. Material Parameters	28
4.9. Fatigue Database	29
4.9.1. Selection Process	29
4.9.2. Determination of Missing Parameters	29
4.10. Stress-Cycle From Industry	31
5. Results	33
5.1. Determination of Parameters	33
5.2. Failure Assessment Diagrams	34
5.3. Predictions for Tests at the Fatigue Limit	35
5.3.1. Predictions for Selected Loading Cases	35
5.3.2. Comparison of Predictions for Material Groups	40
5.4. Stress-Cycle of Dynamically Loaded Component	43
6. Discussion	47
6.1. Requirements of a Fatigue Criterion	47
6.2. Assessment and Suitability of Criteria	48
6.2.1. Normal Stress Criterion	48
6.2.2. Mises-Sines Criterion	49
6.2.3. Tresca-Sines Criterion	49
6.2.4. ASME-Criterion	49
6.2.5. Findley Criterion	50
6.3. Proportional Method vs ASME-Method	50
6.4. Fatigue Assessment of Stress Cycle	52
6.5. A Note on the Availability of Fatigue Test-Data	53
6.6. Continued Work and Suggested Improvements	54
7. Conclusion	57

Contents

Bibliography	59
List of Figures	63
List of Tables	63
A. Material Data	67
B. Predictions	79

1. Introduction

"Structural engineering is the art of modelling materials we do not wholly understand into shapes we cannot precisely analyse so as to withstand forces we cannot properly assess in such a way that the public at large has no reason to suspect the extent of our ignorance."

- Dr. A. R. Dykes [1]

A correct prediction of the fatigue limit and lifetime of a component is of the utmost importance with respect to safety and cost issues. In order to address these challenges, models for fatigue assessment need to accurately predict fatigue-life.

Many mechanical and structural components will throughout their life be subjected to loads of a time-varying nature, with stresses working in several directions. Typical examples are drive shafts in cars, turbine blades in jet engines and windmills. The resulting stress histories may be either proportional or non-proportional, and a number for multiaxial criteria intended for use under such conditions exist. However, the complexity of the fatigue assessment is considerably increased, and so these criteria may be impractical for the practicing engineer. As a result, these criteria are not yet widely implemented. Lately, with the advent of computational resources, the fatigue assessments are made considerably more manageable. Even at the time of writing this thesis, new criteria and algorithms are submitted to the scientific community for review.

This thesis is meant to serve a number of purposes. Primarily, it concerns the fatigue assessment of experimental data collected from the literature. The tests are evaluated using selected criteria, and employed both using a proportional method and with an ASME-inspired method. The results are then presented, and the criteria are compared with respect to usability and accuracy of predictions.

The topic of available experimental data is also addressed, and is an important aspect of this thesis. A thorough search for high cycle fatigue (HCF) tests was conducted, and the results were compiled in a database, spanning 20 different materials and a total of 268 tests. This was necessary in order to provide a comprehensive comparison of the fatigue criteria. Although several such databases are known to

1. Introduction

exist, very few are available for public use. As a result, new criteria are often evaluated for a statistically insignificant number of tests. Several other discrepancies and worrisome trends were encountered during the search, and is critically discussed later on.

Occasionally the gathered tests were incomplete, in that they lacked relevant information regarding the uniaxial fatigue limit σ_A for purely pulsating loading. In these cases, FKM-Richtlinie was used to approximate the mean stress sensitivity M from table-values and known fatigue limits. Since most of the criteria depend on these values, an aspect of this thesis became the quality of FKM-derived values, and their impact on the fatigue assessment.

1.1. Limitation of Investigation

During the investigation, very little fatigue-crack growth data was found. Focus was therefore shifted towards stress-based fatigue criteria and S-N data. The performed analysis spans both shear-stress criteria, and pure normal stress criteria. The shear stress criteria are here represented by the Sines-, Findley- and ASME-criterion. Two versions of the Sines criterion are employed - one with the von Mises equivalent-stress amplitude, and the other with the Tresca equivalent-stress amplitude. The Findley criterion is here applied with the constant k determined by two possible methods. The ASME-criterion as stated in the ASME Boiler and Pressure Vessel Code is included as well. In the normal-stress category, one normal stress criterion based on the Hempel-Morrow line is implemented. All criteria, with the exception of the ASME-criterion are implemented in two different ways. Initially, they are implemented using the traditional, textbook method of assessment. Secondly, an assessment method based on the ASME-criterion is proposed and evaluated.

It was initially intended that non-proportional stress histories *above* the fatigue limit and suitable cycle-counting rules should be considered. Due to limitations in time, it was preferred to expand the database of tests regarding fatigue limits in the high-cycle regime instead. The thesis therefore only concerns local stress based analysis, and mostly plane stresses (2D-stresses).

A fatigue analysis of a dynamically loaded component is provided in order to provide a more comprehensive picture, as opposed to the plane-stress, constant-amplitude stress states provided in the fatigue database.

1.2. Previous Research

Many comparable analyses have been performed by a plethora of authors. Notable contributions in the field are the works of Papadopoulus [2] and Carpinteri [3]. Previous research in the area at NTNU were performed in 1980 by Nøkleby and published in his phd-thesis [4]. Large databases of fatigue limits for proportional and non-proportional loading have been gathered by Papuga on his webpage [5], and by Troost et al. [6]. Experimental data collected from the latter paper have been used in this thesis.

One might conclude that such analyses are neither new nor original, as they have been performed to a great effect by several authors in the past. What sets this thesis apart from similar works is the amount of experimental data used for verification, and the addition of a proposed ASME-inspired assessment method. The data used in this thesis are also enclosed in the appendix. In that respect it might serve as a starting point for future investigations at NTNU.

2. Literature Review

A summary of the literature reviewed is given here. The information provided in this chapter spans from stress analysis, to the fatigue criteria used in the stress analysis. A description of the fatigue database containing collected data is also included in this chapter, but is further explained later on, as several additions (newly calculated parameters) are described in chapter 4 - Procedure.

2.1. Stress Analysis

A comprehensive knowledge of mechanics and stress-analysis is recommended to fully understand the following theory. This section is not an extensive explanation of the subject. It is intended rather, to give a short and clear summary of basic theory needed to implement the fatigue criteria presented in section 2.3. For a more in-depth explanation, the works of Dowling [7] and Marquis, Socie [8] are recommended.

2.1.1. Static Stress Analysis

For the case of 3D-stresses, the stresses at a point \mathbf{x} is given by the Cartesian stress tensor \mathbf{S} given in (2.1),

$$\mathbf{S} = \begin{bmatrix} \sigma_x & \tau_{xy} & \tau_{xz} \\ \tau_{yx} & \sigma_y & \tau_{yz} \\ \tau_{zx} & \tau_{zy} & \sigma_z \end{bmatrix} \quad (2.1)$$

where the equal indexes $i = j$ define a normal stress, and unequal stresses $i \neq j$ define a shear stress. The normal stresses are here given with only one index, i.e x instead of xx due to practicality.

The unit normal vector originating in the point \mathbf{x} , and characterized by the polar angle θ with the y -axis and with the azimuth angle ϕ with the x -axis in a 3D-

2. Literature Review

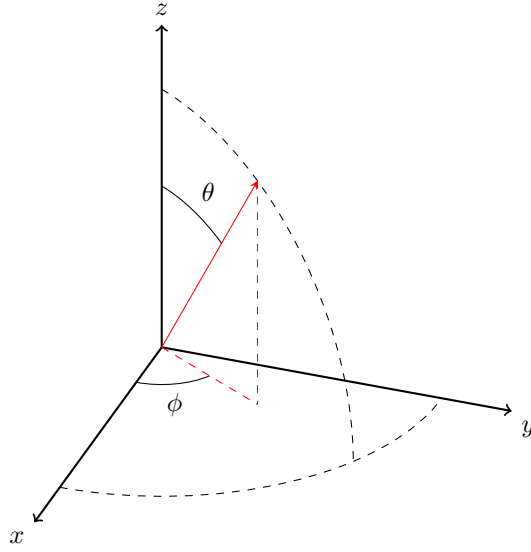


Figure 2.1.1.: 3D-coordinate system.

coordinate system as shown in figure (2.1.1) can be written as

$$\mathbf{n}^T = \begin{bmatrix} \sin\theta\cos\phi & \sin\theta\sin\phi & \cos\theta \end{bmatrix} \quad (2.2)$$

and the tension vector on a plane normal to the vector \mathbf{n} is given by

$$\mathbf{s} = \mathbf{S}\mathbf{n} \quad (2.3)$$

The normal and shear stress on the plane with unit normal vector \mathbf{n} become

$$\sigma = \mathbf{n}^T\mathbf{s} = \mathbf{n}^T\mathbf{S}\mathbf{n} \quad \boldsymbol{\tau} = \mathbf{s} - \sigma\mathbf{n} \quad (2.4)$$

The magnitude of the shear stress vector $\boldsymbol{\tau}$ given in (2.4) can be computed as given by (2.5).

$$\tau^2 = \boldsymbol{\tau}^T\boldsymbol{\tau} = (\mathbf{s} - \sigma\mathbf{n})^T(\mathbf{s} - \sigma\mathbf{n}) = \mathbf{s}^T\mathbf{s} - \sigma^2 \quad (2.5)$$

The principal stresses σ_1 , σ_2 and σ_3 for a 3D-state of stresses are found by solving equation (2.6) with respect to σ .

$$\begin{aligned} \sigma^3 - \sigma^2(\sigma_x + \sigma_y + \sigma_z) + \sigma(\sigma_x\sigma_y + \sigma_y\sigma_z + \sigma_x\sigma_z - \tau_{xy}^2 - \tau_{yz}^2 - \tau_{xz}^2) \\ - (\sigma_x\sigma_y\sigma_z + 2\tau_{xy}\tau_{yz}\tau_{zx} - \sigma_x\tau_{yz}^2 - \sigma_y\tau_{zx}^2 - \sigma_z\tau_{xy}^2) \end{aligned} \quad (2.6)$$

2.1.2. Dynamic Stress Analysis

For stresses varying over time, the stress state can be expressed by introducing the parameter $P(t)$ describing the load history over time. Each of the stress components in \mathbf{S} from (2.1) now take the form of equation (2.7).

$$\sigma_{ij}(\mathbf{x}, t) = P(t)\Sigma_{ij}(\mathbf{x}) \quad (2.7)$$

where \mathbf{x} designates at which point the stresses are working, t is the point in time and $\Sigma_{ij}(\mathbf{x})$ is the stress field in point \mathbf{x} for $P = 1$. A basic alternating and cyclic stress state based on a sinusoidal wave is possibly the easiest case of time varying stresses. The parameter $P(t)$ can be expressed as a sinusoidal wave function when written as $P(t) = P_m + P_a \sin(\omega t)$. For *proportional loading*, the stress components given in \mathbf{S} all vary with the same ratio. This corresponds to the same $P(t)$ valid for all components of \mathbf{S} , so that each of the components may be expressed by equation (2.8),

$$\sigma_{ij}(\mathbf{x}, t) = \sigma_{ij,m}(\mathbf{x}) + \sigma_{ij,a}(\mathbf{x})\sin(\omega t) \quad (2.8)$$

where $\sigma_{ij,m}$ is the mean stress, $\sigma_{ij,a}$ is the stress amplitude and ω is the angular frequency. Since the same ω applies for all stress components, the loading is proportional. As a result, the principal stresses maintain a fixed position with the x , y and z -axis.

The concept of *non-proportional loading* can be explained by introducing angular frequencies ω_{ij} and phase-shifts α_{ij} for each individual component in \mathbf{S} . The parameter describing the load history now takes the form of $P_{ij}(t) = P_m + P_a \sin(\omega_{ij}t - \alpha_{ij})$, with the stress components given as

$$\sigma_{ij}(\mathbf{x}, t) = \sigma_{ij,m}(\mathbf{x}) + \sigma_{ij,a}(\mathbf{x})\sin(\omega_{ij}t - \alpha_{ij}) \quad (2.9)$$

The ratio between the stress-components may now vary with time, and the principal stresses can change orientation. Other variations of non-proportional loading might occur when $P_{ij}(t)$ is a completely random value.

For constant-amplitude loading described in equation (2.8) and (2.9), the cyclic amplitude stress and the constant mean stress can be found from (2.10) and (2.11),

$$\sigma_a = \frac{1}{2}[\sigma_{\max} - \sigma_{\min}] \quad (2.10)$$

$$\sigma_m = \frac{1}{2}[\sigma_{\max} + \sigma_{\min}] \quad (2.11)$$

2. Literature Review

where σ_{\max} and σ_{\min} are the maximum and minimum values of the stress component occurring throughout a cycle. The stress ratio R between the maximum and minimum values is given as

$$R = \frac{\sigma_{\min}}{\sigma_{\max}} \quad (2.12)$$

and thus for fully reversed stresses with $\sigma_{\min} = -\sigma_a$ and $\sigma_{\max} = \sigma_a$ the R-ratio is equal to -1 . For purely pulsating stresses with $\sigma_{\min} = 0$, the ratio $R = 0$.

2.1.3. Special Case of Plane Stress

The case of plane stress is specifically described here as all cases calculated further on are valid for $\sigma_z = 0$ and $\theta = \frac{\pi}{2}$. The principal stresses previously now take on the less challenging form given in (2.13).

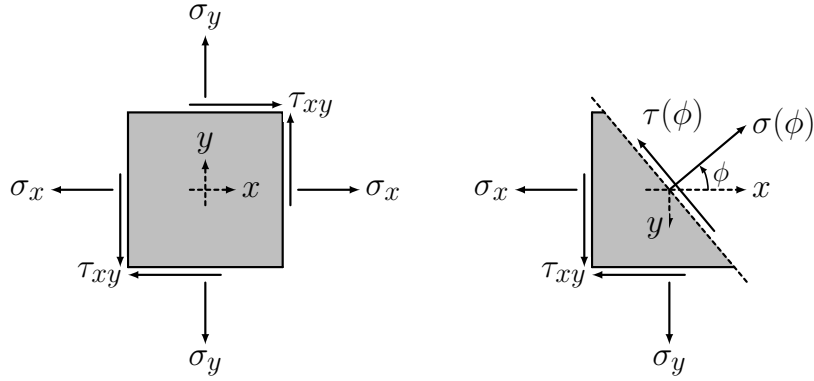


Figure 2.1.2.: Element showing stress components for plane stress, $\sigma_z = 0$.

$$\sigma_{1,2} = \frac{\sigma_x + \sigma_y}{2} \pm \sqrt{\left(\frac{\sigma_x - \sigma_y}{2}\right)^2 + \tau_{xy}^2} \quad (2.13)$$

With the angle $\hat{\phi}$ between the largest principal stress σ_1 and the x-axis given in (2.14).

$$\hat{\phi} = \frac{1}{2} \arctan\left(\frac{2\tau_{xy}}{\sigma_x - \sigma_y}\right) \quad (2.14)$$

The normal stresses (2.15) and (2.16) modified for plane stress are given as

$$\sigma(\phi) = \sigma_x \cos^2 \phi + \sigma_y \sin^2 \phi + 2\tau_{xy} \sin \phi \cos \phi \quad (2.15)$$

$$\tau(\phi) = (\sigma_y - \sigma_x) \sin \phi \cos \phi + \tau_{xy} (\cos^2 \phi - \sin^2 \phi) \quad (2.16)$$

2.2. Uniaxial Fatigue Analysis

Fatigue assessment is the analysis of damage caused by varying stresses over time. The allowable cyclic stresses in order to avoid fatigue failure are determined by the fatigue limit, which are dependent on the material. In the literature it is differentiated between shear stress criteria, and normal stress criteria - each type utilizing a different fatigue limit. For plane stress, a failure locus depicting the boundaries of failure can be drawn, see figure (2.2.1).

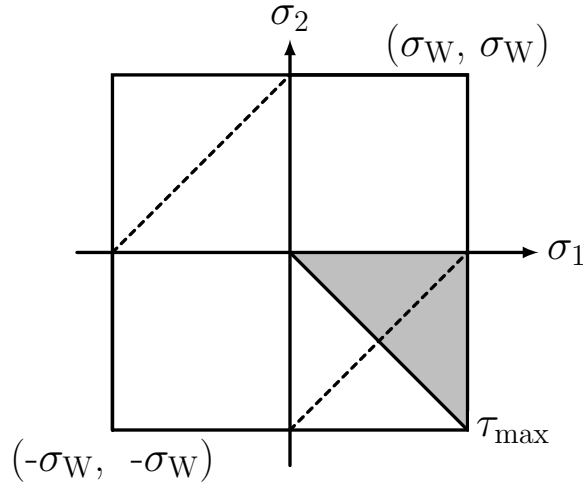


Figure 2.2.1.: Failure locus showing the fatigue limits for fully reversed stresses in shear and normal stress.

The grey area in figure (2.2.1) show the boundaries between a pure shear stress case, and a pure normal stress case. According to the principal stress criteria, a fully reversed normal stress amplitude must be beneath the fatigue limit of the material for fully reversed stresses, σ_W . The shear stress criterion states that the fatigue limit in shear for $R = -1$ is equal to one half of the fatigue limit for normal stress, $\tau_W = \frac{1}{2}\sigma_W$.

The uniaxial fatigue limit for a uniaxial stress cycle with amplitude- and mean stresses can be written as the Hempel-Morrow line given in (2.17),

$$\frac{\sigma_a}{\sigma_W} + \frac{\sigma_m}{\sigma'_f} = 1 \quad (2.17)$$

where σ'_f is a constant. Equation (2.17) is plotted in the Haigh-diagram provided in figure (2.2.2), along with lines for several stress-ratios.

The mean stress sensitivity M , which expresses how sensitive the fatigue limit for purely pulsating stresses, σ_A is to mean stresses is given by equation (2.18) and

2. Literature Review

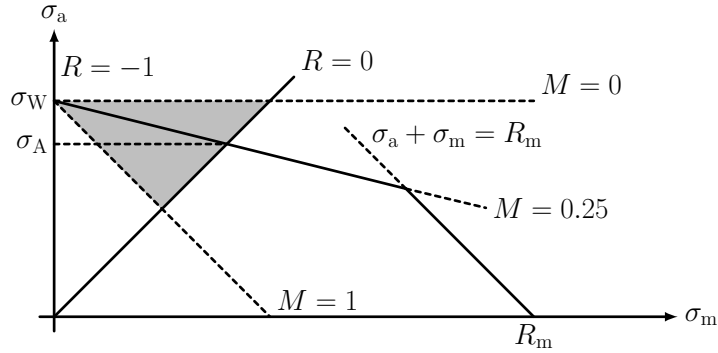


Figure 2.2.2.: Haigh-diagram.

plotted in the Haigh-diagram as well.

$$M = \frac{\sigma_W}{\sigma_A} - 1 \quad (2.18)$$

Equation (2.18) is valid for fatigue limits in both shear and normal stresses. It is however in this thesis only used in combination with the fatigue limits of normal stress.

2.3. Multiaxial Fatigue Criteria

The fatigue models presented here are all on the form given in equation (2.19), and follows the equivalent stress approach where an equivalent stress amplitude σ_{ar} is calculated from multiaxial stresses.

$$\sigma_{ar} = f(\sigma_{ij}, \dots) \leq \sigma_W \quad (2.19)$$

It follows that σ_{ar} is the equivalent uniaxial, fully reversed stress amplitude determined by the function f , which depends on the criteria and the combination of stresses $f(\sigma_{ij}, \dots)$. The determination of σ_{ar} is dependent on the individual criterion. When σ_{ar} is found, it can be compared with σ_W , and failure is predicted when σ_{ar} surpasses σ_W .

The criteria utilized in this thesis are either normal-stress criteria or shear stress criteria. They can further be divided into critical-plane criteria, stress-invariant criteria, and principal-stress based criteria.

2.3.1. Normal Stress Criterion

The simplest criterion presented here is the normal stress criterion [9]. By combining the Hempel-Morrow line given in (2.17) with the mean stress sensitivity M (2.18), the criterion can be shown to be expressed as

$$\sigma_{\text{ar}} = \max[\sigma_{\text{a}}(\phi) + M\sigma_{\text{m}}(\phi)] \leq \sigma_{\text{W}} \quad (2.20)$$

As is apparent from (2.20), only normal stresses on an arbitrary plane are examined. For constant amplitude stresses, both the amplitude and mean stress component throughout the whole cycle are used. Fatigue failure is expected to occur on the plane exposed to the largest combination of stresses. Thus, the plane which maximises the expression $\sigma_{\text{a}}(\phi) + M\sigma_{\text{m}}(\phi)$ is defined as the critical-plane, and the corresponding angle between the x -axis and normal vector \mathbf{n} orthogonal to the plane is designated ϕ_{crit} (for plane stresses).

2.3.2. Mises-Sines Criterion

Sines proposed a criterion intended for in-phase multiaxial proportional stresses in the 1950s [10]. The criterion as it is used here is given in (2.21),

$$\sigma_{\text{ar}} = \max[\sigma_{\text{eq,a}} + MI_1] \leq \sigma_{\text{W}} \quad (2.21)$$

with σ_{eq} being the von Mises equivalent stress amplitude expressed as

$$\sigma_{\text{eq,a}} = \sqrt{\sigma_{x\text{a}}^2 + \sigma_{y\text{a}}^2 - \sigma_{x\text{a}}\sigma_{y\text{a}} + 3\tau_{xy\text{a}}^2} \quad (2.22)$$

and the first stress invariant I_1 given by

$$I_1 = \sigma_{x\text{m}} + \sigma_{y\text{m}} \quad (2.23)$$

Both I_1 and σ_{eq} are here expressed only for plane stress. Both being stress invariants, their validity for non-proportional out-of-phase stresses must be taken into account.

2.3.3. Tresca-Sines Criterion

A modification of the existing Sines criterion is proposed by Härkegård [9] by using the Tresca equivalent stress amplitude $\sigma_{\text{eq,T,a}} = 2\tau_{\text{a,max}}$ instead of the von Mises

2. Literature Review

stress amplitude.

$$\sigma_{\text{ar}} = \max[2\tau_a(\phi)] + MI_1 \leq \sigma_{\text{W}} \quad (2.24)$$

In contrast to the Mises-Sines criterion, the shear-stress on an arbitrary plane are examined. Following the previous procedures, the plane which maximises a combination of stresses are found. Since the stress invariant I_1 is equal in all directions, the critical plane coincides with the maximum shear plane throughout a cycle.

2.3.4. ASME-Criterion for Non-Proportional Loading

Two criteria for multiaxial fatigue stress-based analysis are proposed by the ASME (American Society of Mechanical Engineers) Boiler and Pressure Vessel Code. Only the ASME-criterion for non-proportional loading is presented here, the other one being valid for proportional loading only and the two being identical for such cases. The criterion as it is stated here is taken from [11] and [8].

The ASME-criterion for non-proportional loading may be expressed as follows:

1. Calculate the values for each of the six stress components given in the stress tensor \mathbf{S} , (2.1) over time.
2. Determination of a point in time $\hat{t} = [0, T]$, where the conditions are extreme and T is the length of the stress-history. If this point in time is not known a priori, several points in time need to be examined in order to find the one that yields the largest alternating stress-amplitude σ_{ar} .
3. Determine the stress difference between the stress components in \mathbf{S} occurring at \hat{t} and every other possible point in time $t = [0, T]$. This is done by subtracting the stress-value occurring at \hat{t} from the stress values occurring at t . The resulting stress component is called σ'_{ij} .

$$\sigma'_{ij} = \sigma_{ij}(t) - \sigma_{ij}(\hat{t}) \quad (2.25)$$

4. Calculate the modified principal stresses σ'_1, σ'_2 derived from the six components σ'_{ij} for each point of time during the cycle. Equation (2.13) is used for plane stresses.
5. Determine the stress differences $S'_{12} = \sigma'_1 - \sigma'_2$, $S'_{23} = \sigma'_2 - \sigma'_3$, $S'_{31} = \sigma'_3 - \sigma'_1$ versus time, and find the *largest absolute magnitude* of any stress difference of any point in time. The alternating stress amplitude according to ASME, is

then one half of this magnitude.

$$\sigma_{ar} = \frac{1}{2} \max(|S'_{12}|, |S'_{23}|, |S'_{31}|) \leq \sigma_W \quad (2.26)$$

Nowhere is it specifically stated how to implement the criterion for stress states where non-zero mean stresses are present. Suitable modifications of mean stress are not covered here.

2.3.5. Findley Criterion

The Findley criterion originated in the late 50's is a critical-plane criterion where a linear combination of stresses acting on an arbitrary plane is considered [12]. The general background follows the assumption that shear stresses acting on a plane are the key cause of crack initiation and failure. The maximum normal stress acting on the same plane only amplifies the damaging effect from the shear stresses, and is thus taken into account as well.

The criterion as it was originally presented is given in equation (2.27). The damage parameter f is a function of both shear and normal stress occurring on an arbitrary plane, and thus the critical plane is the plane which maximises the combinations of stresses given in (2.27).

$$f = \max[\tau_a(\phi) + k\sigma_{\max}(\phi)] \leq f_{\text{crit}} \quad (2.27)$$

The constant k and the critical multiaxial fatigue parameter f_{crit} need to be determined by solving (2.27) for at least two uniaxial cases, where only one stress component is present. Input of the corresponding uniaxial fatigue limits for both fully reversed ($R = -1$) and purely pulsating ($R = 0$) yield the four equations (2.28).

$$f = \begin{cases} \frac{\sigma_W}{2} [\sqrt{k^2 + 1} + k] & R = -1 & (2.28a) \\ \frac{\sigma_A}{2} [\sqrt{4k^2 + 1} + 2k] & R = 0 & (2.28b) \\ \tau_W [\sqrt{k^2 + 1}] & R = -1 & (2.28c) \\ \tau_A [\sqrt{4k^2 + 1}] & R = 0 & (2.28d) \end{cases}$$

The parameters k and f_{crit} are then found by setting two of the expressions given in (2.28) equal to each other, i.e $f(\sigma_W) = f(\sigma_A)$ corresponding to equation (2.28b)=(2.28c) and solving for k and f_{crit} .

2. Literature Review

The original criterion can be rewritten as (2.29) using (2.28b), where the f and f_{crit} are replaced by σ_{ar} and σ_{W} . For the sake of comparison, this is the version used in later calculations.

$$\sigma_{\text{ar}} = \max\left(\frac{\tau_{\text{a}}(\phi) + k\sigma_{\text{max}}(\phi)}{\frac{1}{2}(k + \sqrt{1 + k^2})}\right) \leq \sigma_{\text{W}} \quad (2.29)$$

The Findley criterion leaves the user a choice in which fatigue limits one can use to determine the constants k and f_{crit} . Previous examinations (REF) have shown that the combination of these four equations in (2.28) does not yield a unique solution, and since the user may determine the constants based on any two known fatigue limits, k and f_{crit} vary accordingly.

2.3.6. Other Fatigue Criteria

The five previous criteria are only a selection of the wide array of available options. The following sections present additional models for assessing proportional and non-proportional loading, but were not used in the later fatigue assessment.

2.3.6.1. Crossland Criterion

The Crossland criterion [13] is a stress-invariant criterion similar to the Mises-Sines criterion. It uses the von Mises stress amplitude given in (2.22) in combination with the maximum hydrostatic stress $\sigma_{\text{h,max}}$.

$$\sigma_{\text{eq,a}} + \lambda\sigma_{\text{h,max}} \leq \beta \quad (2.30)$$

The constants λ , β are determined by solving the expression (2.22) for simple uniaxial cases and input of the corresponding fatigue limits.

2.3.6.2. McDiarmid Criterion

The McDiarmid criterion [14],[15] utilizes the maximum shear- and normal stress occurring on a plane throughout a cycle. The critical plane is defined as the plane where the largest shear stress amplitude occurs, and not the plane which maximises a combination of stresses (as opposed to the Findley and Normal Stress criterion). The criterion is given in (2.31).

$$\max\left(\frac{\tau_{\text{a}}(\phi)}{\tau_{A,B}}\right) + \frac{\sigma_{\text{a}}(\phi)}{R_{\text{m}}} \leq 1 \quad (2.31)$$

The criterion stands out from the other presented criteria as the shear fatigue strength for either Case A or Case B cracking is used to scale the maximum shear stress. Cracks for Case A propagate parallel along the surface of a component, and Case B cracks propagate into the component from the surface. For combined loading, cracks are developing according to Case A, and $\tau_{A,B}$ is equal to the fatigue limit in shear for fully reversed stresses, $\tau_{A,B} = \tau_W$.

2.3.6.3. Matake Criterion

The criterion proposed by Matake [16] is very similar to the Findley criterion, but differs in the definition of critical plane, which is stated to be the maximum shear plane.

$$\max\{\tau_a(\phi)\} + \lambda\sigma_{\max}(\phi) \leq \beta \quad (2.32)$$

As in the Crossland criterion, the constants λ , β are determined by solving the expression given in (2.32) for uniaxial cases and input of the corresponding fatigue limits. This results in a criterion which is less computationally expensive, as the constants are easier to determine in addition to that the critical plane may be found relatively easy for simple stress states.

2.4. Statistical Analysis

Some statistical parameters are used to better present the results. They are presented as given in [17] and provided here for further reference. The arithmetic mean value \bar{X} of n discrete, random variables are given in (2.33), where X_i is one of n discrete variables.

$$\bar{X} = \frac{1}{n} \sum_{i=1}^n X_i \quad (2.33)$$

The sample standard deviation s is a measure of the degree of spread, and is expressed in (2.34).

$$s = \sqrt{\frac{1}{n-1} \sum_{i=1}^n (X_i - \bar{X})^2} \quad (2.34)$$

2.5. FKM-Richtlinie

FKM-Richtlinie [18, 19] provides solutions and useful experimental approximations of parameters relevant to fatigue assessment. It is mainly used here to determine the

2. Literature Review

mean stress sensitivity M when no σ_A is available. M is given by equation (2.35), with support factors depending on the material provided in table 2.1. It is worth noting that the M is valid for 10^6 cycles.

$$M = a \cdot 10^{-3} R_m + b \quad (2.35)$$

The fatigue limits in shear and normal stresses for fully reversed loading may be approximated by equation (2.36) and (2.37) using tabular values given in table 2.1.

$$\sigma_W = R_m \cdot f_{W,\sigma} \quad (2.36)$$

$$\tau_W = \sigma_W \cdot f_{W,\tau} \quad (2.37)$$

Table 2.1.: Support factors for types of material groups according to FKM-Richtlinie.

Material group	Eng. Translation	$f_{W,\sigma}$	$f_{W,\tau}$	a	b
Einsatzstahl	Unalloyed/low alloy steels	0.40	0.577	0.35	-0.1
Stahl ausser diesen	Other steels	0.45	0.577	0.35	-0.1
GS	Nodular graphite cast iron	0.34	0.577	0.35	0.05
GJL	Lamellar graphite cast iron	0.34	1.0	0.0	0.5
Aluminiumknetwerkstoff	Wrought aluminium	0.30	0.75	1.0	-0.04

The mean stress sensitivity given in (2.35) may be used in combination with the Hempel-Morrow line in equation (2.17) to determine the uniaxial fatigue limit for pure pulsating stress σ_A .

3. Fatigue Test Database

Due to their importance, the fatigue tests assessed in this thesis are presented in a chapter of their own. It contains 268 fatigue limits determined for both combined and uniaxial loading cases. An overview of the materials is given in tables (3.1) and (3.2), together with calculated material parameters relevant to the fatigue assessment.

All fatigue tests are valid for the HCF-regime, with cycles ranging from 10^6 and upwards. The tests were all performed on unnotched, solid or hollow specimens, as specified in table (A.1). The materials are roughly divided into three categories - carbon and low alloy steels, aluminium alloys, and cast irons. The selection process is further explained in section 4.9.

As the fatigue test data collected and assessed in this thesis grew, it became apparent that some assumptions needed to be made. All materials were therefore assumed to be isotropic materials, with no cyclic effects such as isotropic or kinematic hardening.

Perhaps the most influential assumption was the indifference to *loading*, as opposed to the resulting *stresses*. As rotated bending, plane bending, and tension both yield a normal-stress, these were treated as equal. The fatigue limits were however chosen to correspond to the loading case when available. No discrimination was done with respect to the determination of corresponding material parameters from FKM-Richtlinie.

Table 3.1.: Given and calculated material parameters for carbon steels and alloyed steels.

Material	Ref.	Tests		Material parameters from literature					Calculated material parameters		
		given in table	R_m MPa	σ_w MPa	τ_w MPa	σ_A MPa	$\frac{\sigma_w}{\tau_w}$	M	σ_A MPa	$k(\sigma_A)$	$k(\tau_w)$
<i>Carbon- and low alloy steels</i>											
0.1 % C Steel	[20]	A.2	424.6	262.5	149.0	-	0.57	0.049	250.3	0.048	0.136
XC18 Steel	[21]	A.4	520.0	310.0	179.0	-	0.58	0.082	286.5	0.079	0.157
Mild Steel	[3]	A.5	518.8	235.4	137.3	-	0.58	0.082	217.6	0.079	0.169
St35 Steel	[22]	A.6	395	206	123	168.5	0.60	0.223	(198.4)	0.211	0.198
St60 Steel	[6]	A.8	765.2	295	182	264	0.62	0.117	(252.6)	0.113	0.241
Swedish Hard Steel	[3]	A.5	704.1	313.9	196.2	-	0.63	0.146	273.8	0.140	0.258
Clk 35 V	[6]	A.8	706	313	213	245	0.68	0.278	(272.9)	0.264	0.387
C20 annealed Steel	[23]	A.11	520	332	186	-	0.56	0.082	306.8	0.080	0.121
34Cr4 (1)	[22]	A.7	710	343	204	265	0.59	0.294	(298.7)	0.280	0.193
34Cr4 (2)	[22]	A.7	795	410	256	320	0.62	0.281	(348.0)	0.267	0.257
34Cr4 (3)	[22]	A.7	858	415	259	320	0.62	0.297	(345.7)	0.283	0.256
30CrMo16 (1)	[24, 21]	A.4	1160	660	410	-	0.62	0.306	505.4	0.292	0.250
30CrMo16 (2)	[23]	A.11	1200	690	428	-	0.62	0.320	522.7	0.306	0.248
25CrMo4 (1)	[21]	A.4	780	361	228	300	0.63	0.203	(307.8)	0.193	0.273
25CrMo4 (2)	[22]	A.6	780	361	228	300	0.63	0.203	(307.8)	0.193	0.273
S65A	[25]	A.2	1000.8	583.8	370.7	-	0.63	0.250	466.9	0.238	0.280
42CrMo4	[22]	A.6	1025	398	260	310	0.65	0.284	(316.2)	0.270	0.322
25CrMo4 (3)	[6]	A.8	801	340	228	300	0.67	0.133	(288.1)	0.128	0.363
3.5% NiCr steel	[20]	A.3	895.5	540.5	352.1	-	0.65	0.213	445.4	0.202	0.318
34CrMo4 V	[6]	A.9	902	382	283.5	311	0.74	0.228	(314.2)	0.216	0.554

() Stress values are calculated for comparability but not used in later calculations.

Table 3.2.: Given and calculated material parameters for aluminium alloys and cast irons.

Material	Ref.	Tests given in table	Material parameters from literature			Calculated material parameters					
			R_m MPa	σ_w MPa	τ_w MPa	$\frac{\sigma_A}{\tau_w}$	M	σ_A MPa	$k(\sigma_A)$	$k(\tau_w)$	
<i>Aluminium alloys</i>											
76S-T61 (1)	[26]	A.10	499.9	217.9	143.4	-	0.66	0.460	149.2	0.460	0.332
76S-T61 (2)	[26]	A.10	499.9	188.2	119.3	-	0.63	0.438	130.9	0.433	0.278
76S-T61 (3)	[26]	A.10	499.9	170.3	109.6	-	0.64	0.396	122.0	0.386	0.300
<i>Nodular graphite cast irons</i>											
“Sial” cast iron	[20]	A.3	230.1	230.1	199.2	-	0.87	0.161	198.2	0.153	1.073
EN-GJS800-2	[23]	A.11	795	294	220	-	0.75	0.358	216.5	0.345	0.572
<i>Lamellar graphite cast irons</i>											
GG30	[6]	A.9	294	148	135	102.5	0.91	0.444	(98.7)	0.441	1.456
Cast iron	[3]	A.5	230	96.1	91.2	-	0.95	0.500	64.1	0.509	2.041

() Stress values are calculated for comparability but not used in later calculations.

4. Procedure

4.1. General Procedure for Fatigue Assessment

The procedure for the fatigue assessment of proportional and non-proportional stresses may differ depending on the criterion. In order to evaluate all criteria simultaneously, a general algorithm was needed. An overview of the algorithm such as it was implemented is given below. Some steps are elaborated further in the following sections. The algorithm is described for the special case of plane stress, but may be expanded to involve three-dimensional stresses with minimal effort.

1. Determination of any material parameters relevant for the fatigue assessment. This involved constants, fatigue limits and mean stress sensitivity-values.
2. Determination of the three stress components σ_x , σ_y and τ_{xy} , over time. In this case, the stress history was either provided beforehand, or was modelled as a constant-amplitude sinusoidal function.
3. Computation of the principal stresses σ_1 and σ_2 given in (2.13) over time.
4. Calculation of the stresses $\sigma(\phi)$, $\tau(\phi)$ given in (2.15) and (2.16) on every plane $\phi \in [0, 180^\circ]$ with a step of 1° over the course of the whole stress history.
5. Calculation of stress amplitudes σ_{xa} , σ_{ya} , τ_{xya} , $\sigma_a(\phi)$, $\tau_a(\phi)$, and the mean stresses σ_{xm} , σ_{ym} , τ_{xym} , $\sigma_m(\phi)$, $\tau_m(\phi)$.
6. Computation of stress terms such as the stress invariant I_1 from (2.23) and the von Mises equivalent stress amplitude (2.22).
7. Evaluation of the fatigue criteria from all relevant values determined in the previous steps.

This general algorithm describes the steps followed in order to evaluate all criteria utilized here. It follows that some steps are redundant for some, as the computation of I_1 is essential for Mises-Sines and Tresca-Sines, but not necessary for the Findley criterion.

4. Procedure

4.2. Normalizing of Stresses

The fatigue criteria presented in section 2.3 can all be normalized with respect to σ_W . All criteria can now be rewritten according to equation (4.1).

$$\frac{\sigma_{ar}}{\sigma_W} \leq 1 \quad (4.1)$$

The predictions provided by the criteria are now dimensionless, where failure is predicted when $\frac{\sigma_{ar}}{\sigma_W} > 1$. Further it can be shown that the coordinate stresses used as input now take the form of normalized values $\frac{\sigma_x}{\sigma_W}$, $\frac{\sigma_y}{\sigma_W}$ and $\frac{\tau_{xy}}{\sigma_W}$. Advantages when normalizing stresses in this way is the ability to directly compare predictions between different materials and criteria. An added bonus is the more intuitive presentation of the magnitude of a stress-value *relative* to the fatigue limit.

4.3. Determination of Material Parameters and Constants

FKM-Richtlinie was used to determine the mean stress sensitivity M for cases where it was previously unknown. M was calculated by using appropriate constants for the materials, given in table 2.1 and equation (2.35). The fatigue limit for purely pulsating loading σ_A could then be computed using M in combination with (2.18).

The Findley constant k was determined by using the fully reversed fatigue limit σ_W in combination with either σ_A or τ_W . They were calculated using the corresponding equations given in (2.28), so for k determined with the two normal stress fatigue limits, equations (2.28b) and (2.28c) were used. The determined parameters are given as either $k(\sigma_A)$ or $k(\tau_W)$, where σ_A and τ_W denotes which fatigue limits in addition to σ_W were used.

4.4. Modelling of Stress Histories

The fatigue test data compiled in chapter 3 were all reported to originate from investigations where the loading was modelled as a sinusoidal wave with constant-amplitude stresses. The stresses in the calculations are therefore modelled using equation (2.9), here reproduced for ease of access.

$$\sigma_{ij}(\mathbf{x}, t) = \sigma_{ij,m}(\mathbf{x}) + \sigma_{ij,a}(\mathbf{x})\sin(\omega_{ij}t - \alpha_{ij})$$

4.5. Proportional Method for Determination of Criteria

The non-proportionality of the fatigue tests are caused by various phase shifts α [°]. The angular frequency ω [$\frac{rad}{sec}$] were all reported to be equal for the stress components σ_{ij} , and was set to a value of *one*. The length of the stress history was chosen to include at least 3 cycles. Since the period of a sine wave is given as in equation (4.2),

$$period = \frac{2\pi}{\omega} \quad (4.2)$$

this corresponds to a length $T = 6\pi \text{ sec} \approx 18.8 \text{ sec}$. A length was chosen as $T = 20$ sec, and deemed sufficient both with respect to predictions and computing time. The step was set to 1 seconds, forming a time-vector as $t = \left[0 \ 1 \ \dots \ 20 \right]$ seconds.

The choice of T for constant amplitude stresses has no effect on predictions as long as one full cycle is included in the stress history. It does however have an effect on computing time, as it is desired to compute stresses for as few points in time as possible.

4.5. Proportional Method for Determination of Criteria

Most of the criteria presented here are deduced for proportional, constant amplitude loading. The determination of the mean and alternating stress components is based on maximum and minimum values of the stresses, occurring *throughout the whole cycle*, as given in equation (2.11) and (2.10). For non-proportional loading, the maximum and minimum values used to determine the amplitudes and mean stresses may occur at severely different points in time, and thus the variations in stresses (local maxima and minima) may not be taken sufficiently into account. This method is hereby referred to as the *proportional method*, as opposed to the proposed *ASME-method* for determination of stress parameters presented in the following section.

4.6. ASME Method for Determination of Criteria

The proportional-method of assessing the criteria deals with constant-amplitude loading. An alternative method inspired by the ASME-criterion for assessing multi-axial fatigue criteria is proposed, where the parameters used for fatigue calculation are determined for a restricted interval in time. The stress-parameters defined on each interval are hypothesised to have a specific relevance to each other, and thus yielding more accurate predictions.

4. Procedure

1. Compute the six stress components σ_x, σ_y etc. given by the Cartesian stress tensor \mathbf{S} for the whole cycle or stress history. The length of the stress history measured in seconds can be denoted T .
2. Divide the resulting stress histories into steps, i.e steps of 1 second each when dealing with a stress history measured in seconds. When dealing with sinusoidal-functions, steps of radians may also be used.
3. The ASME-criterion states that a point in time where the conditions are extreme should be chosen, or when these are not easily identifiable that several points in time should be tried. When using the ASME-inspired assessment method however, combinations of parameters contained in each individual criterion influence the $\frac{\sigma_{ar}}{\sigma_w}$. As a result it might be challenging to pinpoint which points in time corresponds to the maximum prediction value. It is highly recommended that every possible combination is tried and tested. The point in time where the conditions are extreme can be denoted \hat{t} , and can be described by the vector $\hat{t} \in [0, T]$.
4. The stress parameters used by the criteria are then calculated for each potential critical point \hat{t} relative to each point in time $t \in [\hat{t}, T]$. The stress parameters are computed based on the stresses at the end points of the interval $[\hat{t}, t]$. Stress amplitudes and mean stresses are calculated according to (4.3) and (4.4). Notice that the absolute value of the stress difference is used when amplitudes are evaluated.

$$\sigma_a(\hat{t}, t) = \frac{1}{2}|\sigma(\hat{t}) - \sigma(t)| \quad (4.3)$$

$$\sigma_m(\hat{t}, t) = \frac{1}{2}[\sigma(\hat{t}) + \sigma(t)] \quad (4.4)$$

Maximum and minimum stresses on the interval $[\hat{t}, t]$ are found as

$$\sigma_{\max} = \max[\sigma(\hat{t}), \sigma(t)] \quad (4.5)$$

$$\sigma_{\min} = \min[\sigma(\hat{t}), \sigma(t)] \quad (4.6)$$

5. The calculated stress components may be placed in matrixes where \hat{t} is the number of rows and t is the number of columns. Such a matrix is here exemplified

for stress-amplitudes.

$$\boldsymbol{\sigma}_{ij,a}(\hat{t}, t) = \begin{bmatrix} \sigma_{ij,a}(0, 0) & \sigma_{ij,a}(0, 1) & \cdots & \sigma_{ij,a}(0, T) \\ \vdots & \sigma_{ij,a}(1, 1) & & \\ \vdots & & & \\ \sigma_{ij,a}(T, 0) & & & \sigma_{ij,a}(0, T) \end{bmatrix} \quad (4.7)$$

6. Other parameters such as the stress invariant I_1 are also calculated interval-wise, so that $I_1(\hat{t}, t) = \sigma_{xm}(\hat{t}, t) + \sigma_{ym}(\hat{t}, t)$ for plane stress. The same goes for the von Mises stress amplitude $\sigma_{eq,a}$.
7. When dealing with critical-plane criteria where the critical plane is unknown, the relevant stress parameters occurring on $\phi \in [0, 180^\circ]$, i.e. $\sigma_{\max}(\phi)$, $\tau_a(\phi)$ (for plane stress) need to be determined interval-wise as described in step 4.
8. The fatigue criteria may now be evaluated for every interval when all relevant mean-values, amplitudes, maximum and minimum values are calculated for every combination of $\hat{t} \in [0, T]$ and $t \in [\hat{t}, T]$. An example is provided using the Mises-Sines criterion.

$$\sigma_{ar} = \max_{(\hat{t}, t)} [\boldsymbol{\sigma}_{eq}(\hat{t}, t) + M\mathbf{I}_1(\hat{t}, t)] \leq \sigma_w \quad (4.8)$$

The combination of $[\hat{t}, t]$ yielding the largest σ_{ar} , denoted $\sigma_{ar, \max}$ is then assumed to give the largest contribution to fatigue damage.

This method can be utilized for a wide range of criteria, both those based on stress-invariants and critical-planes. It does however require a large amount of calculations to be done. It is especially challenging for the criteria where the criterion needs to be evaluated for every interval, on every possible plane.

4.7. Computational Algorithm

The calculations done in this thesis were many and often extensive. The sheer amount of calculations meant that this task would be better executed by software. The several types of software were chosen out of availability, and previous experience.

Microsoft Excel 2011 was used to store, and to a degree sort the collected data. Solving of intricate equations were done in the technical computing software Maple, version 16. For the major calculations, MATLAB R2013a was used. MATLAB

4. Procedure

has the ability to read and write values from Excel, and this close integration was necessary in order to effectively evaluate the test data.

It was decided that a modular approach, with several interlinking scripts and each one performing a distinctive task, provided the best overview. A modular build was decided upon, where several individual scripts were linked together. This ensured a transparent process, where each script had only *one* specific task to fulfil. The scripts utilized can be grouped into two categories, *main-scripts* and *supporting-scripts*. The main scripts were responsible for compiling the essential functions needed in order to perform the fatigue assessment as a whole. The support-scripts each had a specific function to fulfil, and were called by the main-scripts when needed.

Material Database This was a large excel document where fatigue tests collected from the literature were assembled. Information about stresses, stress-ratios, material constants etc. were pre-calculated and inserted into the database.

Support 1 - SORT The SORT script, loaded values and information from the material database into MATLAB. It then and sorts all the fatigue tests according to a pre-set preference, i.e all tests where $R_x = -1$ and $\alpha_{xy} = 0^\circ$. The preferences could be changed according to specific needs.

Support 2 - CALC I This script uses input values provided from one of the four main scripts to construct a stress history. The stress history is then evaluated using the fatigue criteria and their *original method of assessment*. It is designed so that it may run in a loop, which is required from both the FAD and the FATDATA-script. The calculated values are then exported back to a main script.

Support 3 - CALC II This script worked the same way as CALC I, but the tests were evaluated using the *ASME-method* to assess the stress history.

Main script 1 - BASIC This is the simplest script utilized. It is mainly used to check single fatigue tests with control calculations, and also to determine specific stress combinations. It requires input of material parameters, and links to the calculation-script (CALC). The results may then plotted.

Main script 2 - FAD The script uses either of the support scripts CALC I and II in a loop for various combinations of normalized coordinate stresses. The results are plotted as the diagrams shown in section 5.2.

Main script 3 - FATDATA The FATDATA-script retrieves values from the SORT-script, then evaluates each of them using CALC I or II run in a loop. The mean value and standard deviation of predictions from the criteria are then calculated.

Main script 4 - STRESSHIST The STRESSHIST-script loads a previously known stress history from Excel into MATLAB. It links to CALC I or II for assessment.

4.8. Failure Assessment Diagrams

A visual presentation of a fatigue criterion provided on the normalized form given in (4.1) can be made by calculating the $\frac{\sigma_{ar}}{\sigma_W}$ -values for combinations of the normalized stress components $\frac{\sigma_{xa}}{\sigma_W}$, $\frac{\sigma_{xm}}{\sigma_W}$, $\frac{\tau_{xya}}{\sigma_W}$, $\frac{\tau_{xym}}{\sigma_W}$, and plotting a line corresponding to a chosen $\frac{\sigma_{ar}}{\sigma_W}$ -value. At the fatigue limit σ_W , this value is equal to one and the plotted line corresponds to the limiting state of non-failure predicted by the criterion. Diagrams of this type are hereby referred to as failure assessment diagrams (FAD). The area beneath the curve represents all combinations of coordinate stresses predicted to *not* cause fatigue failure. An example of such a diagram is given in figure 4.8.1.

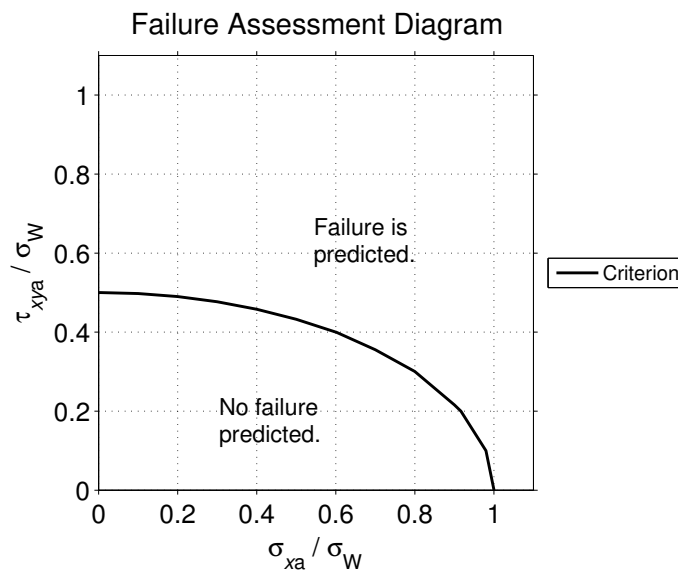


Figure 4.8.1.: Example of a failure assessment diagram for the Tresca-Sines criterion.

4. Procedure

The biaxial fatigue limits collected in the material database can, when normalized, be plotted in a FAD along with a criterion. For a criterion that correctly predicts fatigue behaviour, the plotted fatigue limits are expected to lie on, or in the immediate vicinity of the plotted line. Fatigue limits from experimental data, which when plotted lie *beneath* the curve, show graphically that the prediction done by the criterion is non-conservative. Subsequently, a plotted fatigue limit *above* the curve corresponds to a conservative prediction.

4.8.1. Algorithm and Plotting

As previously mentioned, the FAD's were plotted by calculating the corresponding $\frac{\sigma_{ar}}{\sigma_W}$ for a combinations of the normalized coordinate stresses. The values for the amplitude and mean stress components were chosen to range from 0 to 1.1 with a step of 0.1 as given in equation (4.9). Each combination of stresses was calculated by the FAD-script described in section 4.7 using the general algorithm provided in section 4.1.

$$\frac{\sigma_{ija}}{\sigma_W} = \left[0 \quad 0.1 \quad \dots \quad 1.1 \right] \quad \frac{\sigma_{ijm}}{\sigma_W} = \left[0 \quad 0.1 \quad \dots \quad 1.1 \right] \quad (4.9)$$

The length of the row matrix given in (4.9) is 12, and for the case of $R = -1$ valid for one alternating normal stress together with one alternating shear stress, $12 \cdot 12 = 144$ combinations exist. For each criterion, the value of the calculated $\frac{\sigma_{ar}}{\sigma_W}$ was inserted into a 12 by 12 matrix. An iso-line with a value of one was then plotted using the contour-function in MATLAB. The contour-function automatically finds the critical combinations of stresses yielding σ_{ar} by interpolation between neighbouring values in the matrix. This was deemed preferable to solving the criteria-equations, and expressing one stress component as a function of another. Especially the equations for the critical-plane criteria would have been challenging to solve.

4.8.2. Material Parameters

One of the benefits of normalizing stress components with respect to σ_W is that they become dimensionless. The stress components $\frac{\sigma_{xa}}{\sigma_W}$ and $\frac{\tau_{xya}}{\sigma_W}$ corresponding to the fatigue limit for combined loading may then be plotted in the same diagram, regardless of materials (different σ_W). When plotting combined fatigue limits (combinations of $\frac{\sigma_{xa}}{\sigma_W}$ and $\frac{\tau_{xya}}{\sigma_W}$) for $R = -1$ in a FAD, the effect of the mean stress sensitivity is removed for most of the fatigue criteria. For the Findley criterion however, the constant k needs to be determined based on σ_W , σ_A and τ_W . As the latter fatigue

limits vary between materials, the mean values $\bar{k}(\sigma_A)$ and $\bar{k}(\tau_W)$ for the three different material groups were used. These are given in table 5.1. The resulting failure assessment diagrams are given in figure 5.2.1, 5.2.2 and 5.2.3.

4.9. Fatigue Database

An extensive search for suitable fatigue tests from the literature was conducted. The search yielded a total number of 268 individual tests spanning 20 materials. It was decided to sort the data into three categories, carbon and low alloy steels, Aluminium alloys, and cast irons. Information about the collected materials and their sources are provided in table 4.1.

4.9.1. Selection Process

The search was restricted to only include fatigue limits in the high cycle regime, which is here defined as 10^6 cycles or more. A fatigue limits/strengths for the lower ranges were ignored. All fatigue limits were reported to be conducted on either solid or hollow unnotched specimens. The majority of tests are determined by either S-N testing or the staircase method, although information is lacking regarding some of them. An overview is given in table 4.1. Fatigue limits for pure uniaxial cases were included where available.

Materials are gathered from what was deemed as trustworthy sources. Occasionally when the original paper cited as the primary source was unavailable, data reported in other papers by same authors as the original paper were used. These cases are marked with an asterisk * in table 4.1.

4.9.2. Determination of Missing Parameters

When material parameters relevant for the fatigue assessment were unavailable, these were approximated using FKM-Richtlinie. In large, this meant determining the mean stress sensitivity M and σ_A from equation (2.35) and (2.18), when σ_A was unknown. The constants utilized were gathered from table 2.1. The carbon and low-alloy steels were assumed to belong to the group *einsatzstahl*, while the aluminium alloy 76S-T61 count as an *aluminiumknetwerkstoff*. The two groups of cast irons were *GS* and *GJL*, with constants chosen accordingly.

As previously mentioned, the M determined from FKM-Richtlinie is valid for 10^6 cycles. Many test-series (see table A.1) were reported to apply for $>10^6$ cycles.

4. Procedure

Table 4.1.: List of materials collected from the literature and their references. For some materials, several data sets exist and each individual data set is numbered with a number inside a parenthesis.

Material	Collected from	Primary source	Tests	Remarks
<i>Carbon- and low alloy steels</i>				
0.1%C Steel	[25]	Yes	7	
XC18 Steel	[21]	Yes	5	
Mild Steel	[3]	No, [27]	10	
St35 Steel	[22]	No,[28]	12	
St60 Steel	[6]	No, [29],[30]	7	
Swedish Hard Steel	[3]	No, [27]	12	
Ck 35 V	[6]	No, [31]	11	
C20 Annealed Steel	[23]	No, [32]	3	
34Cr4 (1)	[22]	No,[33, 34, 35]	9	*
34Cr4 (2)	[22]	No,[34, 35]	14	*
34Cr4 (3)	[22]	No,[34, 35]	4	*
30CrMo16 (1)	[24, 21]	Yes	16	
30CrMo16 (2)	[23]	No,[36]	29	*
25CrMo4 (1)	[21]	No,[37]	4	
25CrMo4 (2)	[22]	No,[37]	8	
S65A	[25]	Yes	27	
42CrMo4	[22]	No,[38]	9	
25CrMo4 (3)	[6]	No,[39],[40],[41]	12	*
3.5% NiCr Steel	[25]	Yes	7	
34CrMo4 V	[6]	No, [31]	15	
<i>Aluminium alloys</i>				
76S-T61 (1)-(3)	[26]	Yes	21	
<i>Nodular graphite cast irons</i>				
“Sikal” Cast Iron	[20]	Yes	7	
EN-GJS800-2	[23]	No,[42],[43]	4	*
<i>Lamellar graphite cast irons</i>				
GG30	[6]	No, [31]	7	
Grey Cast Iron	[3]	No, [27]	8	
Sum:			268	

* Overlap of authors between primary source and paper the tests are collected from.
 () Several data sets for each material exists and are numbered accordingly.

Without sufficient information, the FKM-determined M was assumed to be valid for these cases as well. This assumption might prove passable for steels, where the fatigue limits at higher cycles are nearly identical as the slope of an S-N curve flattens out. It is not however justifiable for aluminium alloys, and a special exception was made for the alloy 76S-T61. Since the uniaxial fatigue limits σ_W were provided for 10^6 , 10^7 and 10^8 cycles, different values of M and σ_A were expected for each N_f .

The solution was to calculate the fatigue strength coefficient σ'_f using the Hempel-Morrow line given in equation (2.17) and parameters valid for $N_f = 10^6$. The value of σ'_f was calculated to $\sigma'_f = 429.5$ MPa. Since σ'_f is a constant, σ_A for 10^7 and 10^8 cycles could be determined using equation (2.17), and M from equation (2.18).

4.10. Stress-Cycle From Industry

A fatigue assessment of a typical stress-cycle from the industry was also carried out. Very little information is provided due to protection of confidentiality, and it is chiefly included here to illustrate the fatigue assessment and use of multiaxial criteria for a cycle with variable-amplitude stresses in three dimensions. The stress cycle consisting of the stress components σ_x , σ_y and τ_{xy} normalized with respect to the largest absolute value of the occurring stresses $|\sigma_x|_{\max}$ is given in figure 4.10.1. Selected values of the stresses occurring throughout the cycle is given in table 4.2.

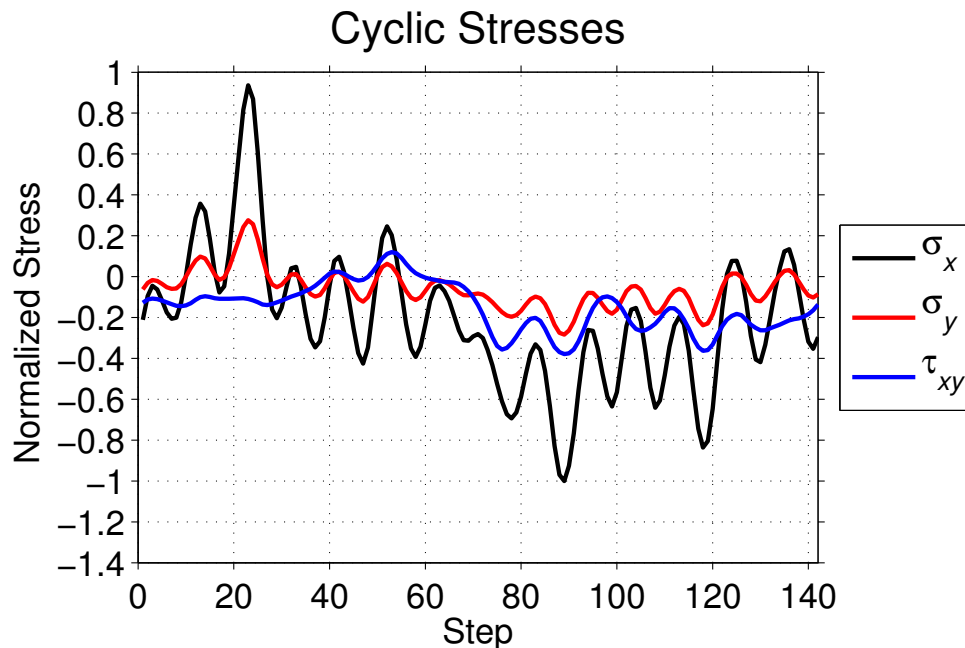


Figure 4.10.1.: Cyclic stresses for dynamically loaded mechanical component.

4. Procedure

Table 4.2.: Extreme values of stresses during a cycle of a dynamically loaded component.

	$\frac{\sigma_{x,\max}}{ \sigma_x _{\max}}$	$\frac{\sigma_{x,\min}}{ \sigma_x _{\max}}$	$\frac{\sigma_{y,\max}}{ \sigma_x _{\max}}$	$\frac{\sigma_{y,\min}}{ \sigma_x _{\max}}$	$\frac{\tau_{xy,\max}}{ \sigma_x _{\max}}$	$\frac{\tau_{xy,\min}}{ \sigma_x _{\max}}$	$\frac{\tau_{xy}}{ \sigma_x _{\max}}$
Value	0.94	-1.00	0.28	-0.28	0.12	-0.38	-0.12
Step	23	89	23	89	53	89	23

As so little was previously known about the cycle, several assumptions were necessary in order to perform the fatigue assessment.

1. The material is assumed to be a *Stahl ausser diesen* with $R_m = 1000$ MPa and fatigue limits and other parameters calculated from FKM-Richtlinie according to section 2.5. The parameters are given in table 4.3.
2. The length of the cycle is given as 142 steps. Assuming the specimen is rotating, an angular step of 2.5° corresponds to $\frac{360^\circ}{2.5^\circ} = 144$ steps, leaving two steps short of a full cycle. It is assumed that the two missing steps do not impact the fatigue assessment. This is supported by the fact that the stresses in step 1 and 142 are close to each other, and relatively far from any influencing global extreme-values.
3. When using the ASME-method, it was assumed that each step corresponds to a point in time with equal difference between two consecutive values. The ASME-method is then used by substituting *points in time* with *steps*.

The Hempel-Morrow line given in (2.17) was used to determine σ_A . The resulting material parameters and fatigue limits are given in table 4.3.

Table 4.3.: Material parameters for a constructed steel according to FKM-Richtlinie and assumed to be valid for the stress cycle given in figure (4.10.1).

R_m (MPa)	σ_W (MPa)	τ_W (MPa)	σ_A (MPa)	M	$k(\sigma_A)$	$k(\tau_W)$
1000	450	259.7	360	0.250	0.237	0.156

5. Results

5.1. Determination of Parameters

The calculated parameters are for comparisons sake given together with the reported material parameters in table 3.1 for carbon/low alloy steels and table 3.2 for Aluminium/cast irons. The degree of appropriateness can to a certain degree be determined by comparing the calculated σ_A with the reported value in cases where this was obtainable. In general, the σ_A calculated from FKM-Richtlinie and the Hempel-Morrow line is larger than the reported value. In this respect, FKM and Hempel-Morrow yield non-conservative results. It is worth noting however, that the true experimentally determined σ_A was only reported for about half of the test series used in the fatigue assessment.

Average values for the material parameters M , $k(\sigma_A)$ and $k(\tau_W)$ used in the fatigue assessment are given for the three material groups in table 5.1.

Table 5.1.: Average values of M , $k(\sigma_A)$ and $k(\tau_W)$ reported in table 3.1 and 3.2 with respect to material grouping. Only values used in the fatigue analysis was counted in.

Material group	\bar{M}	$\bar{k}(\sigma_A)$	$\bar{k}(\tau_W)$
Carbon- and low alloy steels	0.204	0.194	0.263
Aluminium	0.431	0.427	0.303
Cast irons	0.366	0.362	1.286

Comparing the average values, the Findley constant k determined with the fatigue limits σ_W and σ_A lie close to the mean stress sensitivity. There are however a notable difference between the mean values $\bar{k}(\sigma_A)$ and $\bar{k}(\tau_W)$ between material groups.

5.2. Failure Assessment Diagrams

As previously stated, a failure assessment diagram is a visual presentation of a criterion at the fatigue limit. The area under each individual curve represents the safe combinations, where a criterion does not predict failure. Three such diagrams are presented here, with the criteria calculated using the average values for each material group given in table 5.1. The criteria are plotted for fully reversed $R = -1$ stresses, with no phase difference, $\alpha_{ij} = 0^\circ$. Since no mean-stresses are present, the influence of M is negated. For the sake of comparison, Findley evaluated with $k(\sigma_A)$ is left out. Only criteria assessed the traditional way are plotted.

Fatigue test data for the corresponding cases and shear- and normal-stresses are plotted for each material group as well. For the case of uniaxial stresses, only the shear stresses are plotted (points along the $\frac{\tau_{xya}}{\sigma_W}$ -axis). Since the criteria are calculated based on average material parameters, some deviation between the points and the curves is expected.

The FAD for all three material groups are given in table 5.2.1-5.2.3. Some general trends are immediately valid for all material groups. Only the Findley criterion is shown to adapt to the change between fatigue-fracture governed by either normal or shear-stresses, due to k being evaluated by σ_W and τ_W . All the other criteria are the same for all material groups. The Tresca-Sines criterion is identical to the ASME-criterion, and due to this overlap, the ASME-criterion is the only one shown.

The normal stress criterion, which only takes normal-stresses into account predicts a limiting state of non-fracture both at pure shear $\frac{\tau_{xya}}{\sigma_W} = 1$ and for pure normal stress $\frac{\sigma_{xa}}{\sigma_W} = 1$. For fully reversed loading, this is easily explained using principal stresses (equation (2.13)) and it can be shown that the largest alternating amplitude is allowed to be equal to σ_W . The same goes for pure shear stress, as $\sigma_1 = \sqrt{\tau_{xya}^2} = \sigma_W$.

The Mises-Sines criteria predicts for fully reversed normal stress $\sigma_{ar} = \sqrt{\sigma_{xa}^2} = \sigma_W$, and fully reversed shear stress, $\sigma_{ar} = \sqrt{3\tau_{xya}^2} \implies \frac{\tau_{xya}}{\sigma_W} = \frac{1}{\sqrt{3}} = 0.577$. The Tresca-Sines criterion predicts $\sigma_{ar} = 2\tau_{xya} \implies \frac{\tau_{xya}}{\sigma_W} = \frac{1}{2} = 0.5$ for pure shear, and $\sigma_{ar} = 2\tau_{xya} = 2 \cdot \frac{1}{2}\sigma_{1,\max} \implies \frac{\sigma_{xa}}{\sigma_W} = 1$ for pure normal stress. The end points for the Findley criterion are challenging to show in a practical manner due to the critical-plane.

For carbon and low alloy steels plotted in figure 5.2.1, the fatigue test data seem to lie in the vicinity of the shear stress criteria. The predictions for these seem overall to be conservative, while the normal-stress criterion is mainly non-conservative.

As for the carbon and low alloy steels, the fatigue data for aluminium plotted in figure 5.2.2 show a good correlation with the shear criteria. The FAD for cast irons

Criteria and tests for carbon/low alloy steels.

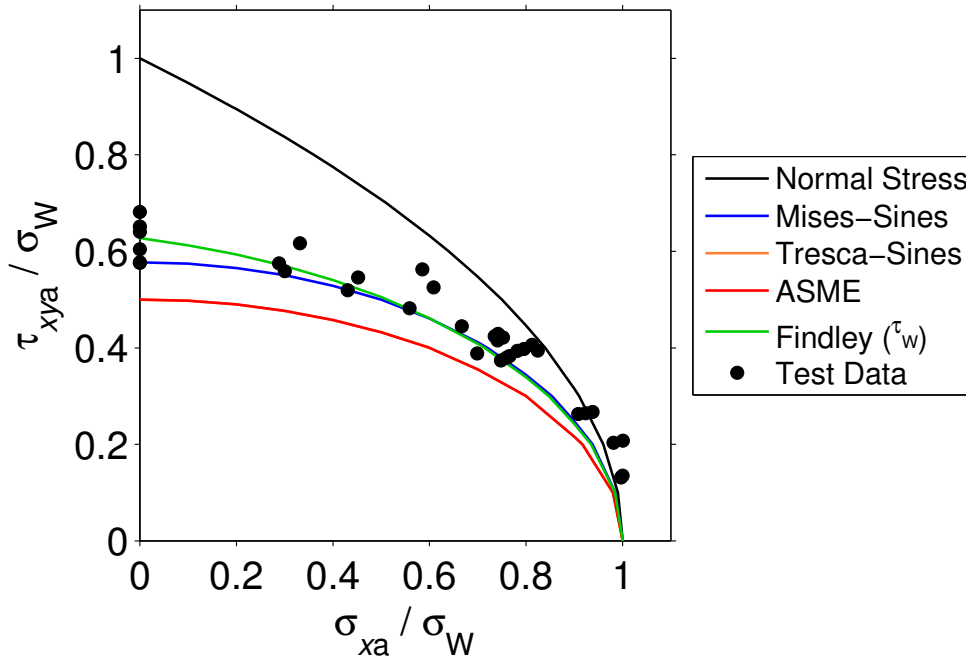


Figure 5.2.1.: Failure assessment diagram, $R = -1$ and $\alpha_{ij} = 0^\circ$. Test data are 34 fatigue tests for carbon/low alloy steels.

given in 5.2.3 show data in good correlation with the normal stress criterion, rather than with the shear stress criteria. Some outliers are present.

5.3. Predictions for Tests at the Fatigue Limit

What follows are the results from the evaluation of the fatigue criteria at the collected tests from the literature. An overview of the data is given in table 3.1 and 3.2, while the data themselves are given in appendix A, tables A.2 to A.11. The predictions for all 268 tests provided in table 5.2 includes all loading cases present. The outcome is also plotted in the histograms 5.3.1 and 5.3.2.

The fatigue tests were grouped according to selected stress states and materials. Both predictions based on traditional criteria and ASME-criteria are presented side by side for the sake of comparison. The predictions are given in table 5.2 and 5.3.

5.3.1. Predictions for Selected Loading Cases

Predictions for several selected stress ratios and variations of loading parameters are given in table 5.2 and 3.1.

5. Results

Criteria and tests for aluminium 76S-T61.

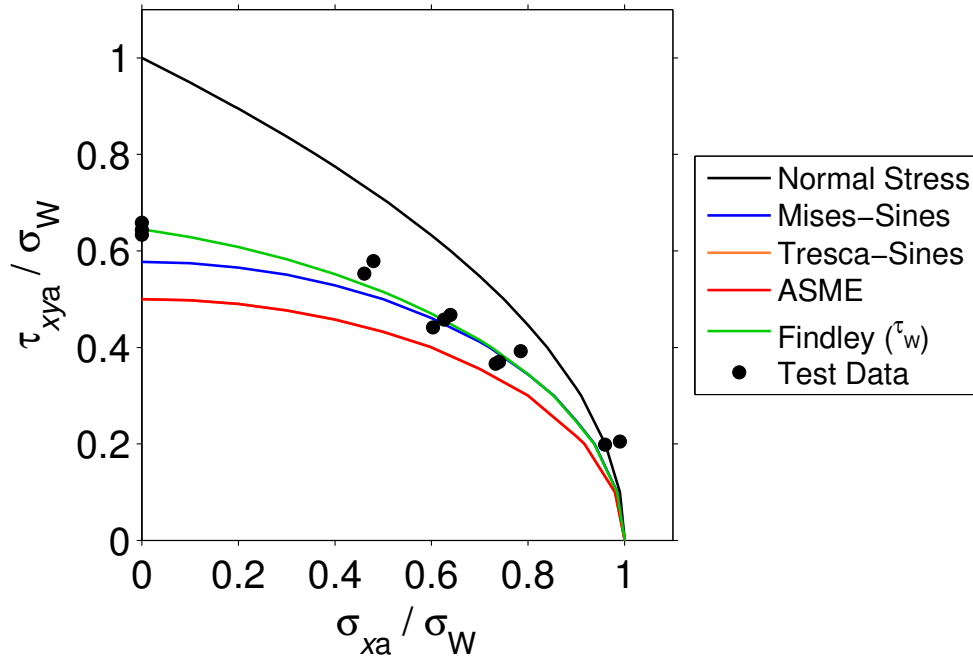


Figure 5.2.2.: Failure assessment diagram, $R = -1$ and $\alpha_{ij} = 0^\circ$. Test data are 13 fatigue tests for 76S-T61.

Criteria and tests for cast irons.

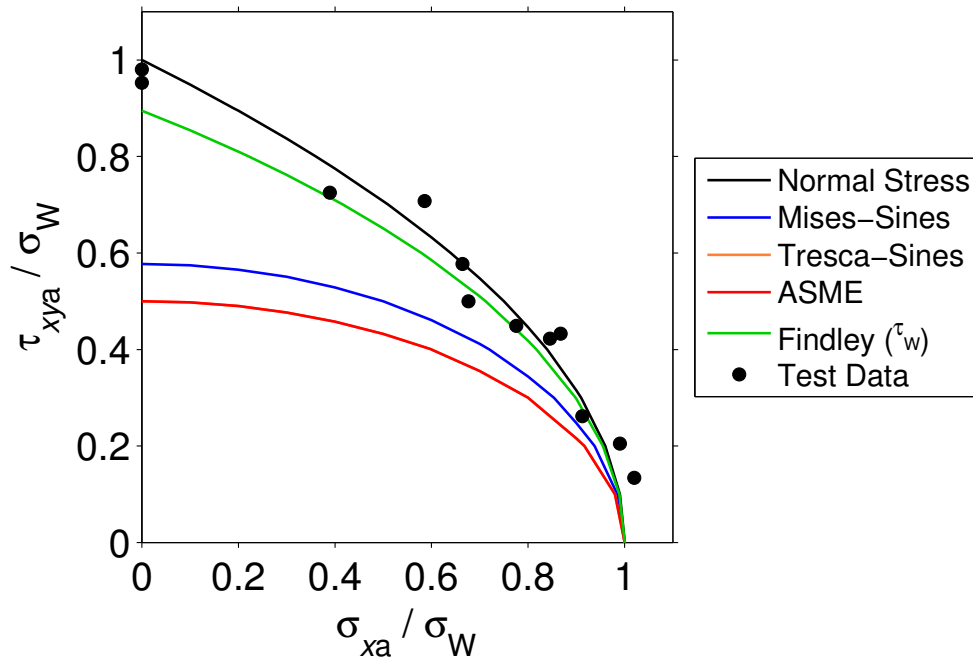


Figure 5.2.3.: Failure assessment diagram, $R = -1$ and $\alpha_{ij} = 0^\circ$. Test data are 12 fatigue tests for cast irons.

5.3. Predictions for Tests at the Fatigue Limit

The normal-stress criterion is the only criterion with overall non-conservative predictions, as the mean value of $\frac{\sigma_{ar}}{\sigma_W}$ lies beneath 1. The criterion performs quite badly when used to assess the 11 tests for fully reversed shear stresses. The standard deviation $s_p = 0.14$ is lower or equal than the standard deviations for other criteria. This indicates that the predictions are gathered relatively close. For the normal stress criterion, no overall difference is found when comparing the ASME-assessment method with the traditional critical plane approach.

The Mises-Sines criterion yields good predictions overall, with predictions slightly on the conservative side. For fully reversed loading with $\alpha_{xy} \neq 0^\circ$, Mises-Sines-ASME yields a mean value beneath 1. For loading with mean stresses without a phase shift, a m_p very close to one is observed for both Mises-Sines and Mises-Sines-ASME. The s_p however is quite high.

The Tresca-Sines criterion has one of the overall largest spread with $s_p = 0.22$ and $s_p = 0.21$ for Tresca-Sines-ASME. Both versions provide highly inaccurate predictions for the pure shear tests. For stresses with $R = -1$ and $\alpha_{xy} \neq 0^\circ$, a large spread in the predictions for both variations of the criterion is observed. The mean value however is very good for Tresca-Sines.

The ASME-criterion stands out with a accurate mean value $m_p = 0.99$. The standard deviation is however quite large signalling a large spread in predictions. For the 11 cases of pure shear, the predictions are highly conservative and inaccurate (large spread). For cases with mean stresses present, the criterion is non-conservative. For stresses with $R = -1$ the ASME-criterion yields the same predictions as Tresca-Sines.

The Findley criterion shows an improvement in mean value m_p when assessed with the ASME-method. This is especially prominent for stresses where $R \neq -1$ without phase shifts. The Findley criterion using $k(\sigma_A)$ yields overall a m_p slightly closer to one than when using $k(\tau_W)$, but the latter performs extremely well for the 11 pure shear-tests. A distinct decrease in mean value occur for Findley-ASME and $R \neq -1, \alpha_{xy} \neq 0^\circ$.

For cases given in table 3.1 where σ_y is taken into account, the predictions for all criteria are generally characterized by a large spread in predictions. The normal stress criterion however, yields similar predictions for a shear stress component with both one and two normal stress components present. The Mises-Sines criterion yields very good predictions, but the results worsen when assessed with the ASME-method. For cases with three stress components, the Findley criterion yields non-conservative predictions with a high degree of spread.

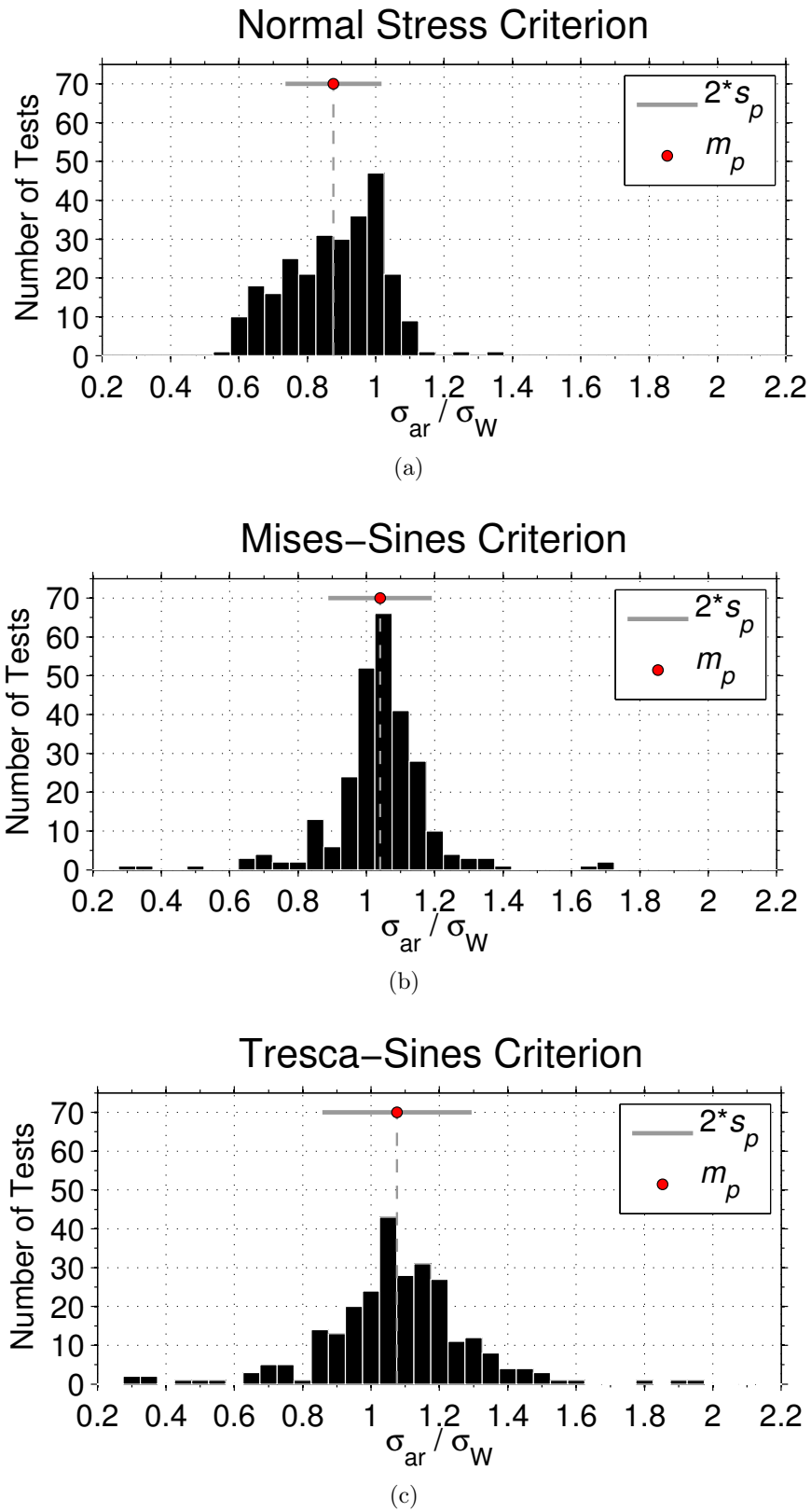


Figure 5.3.1.: Predictions and their distribution for the criteria normal stress, Mises-Sines and Tresca-Sines for all 268 tests.

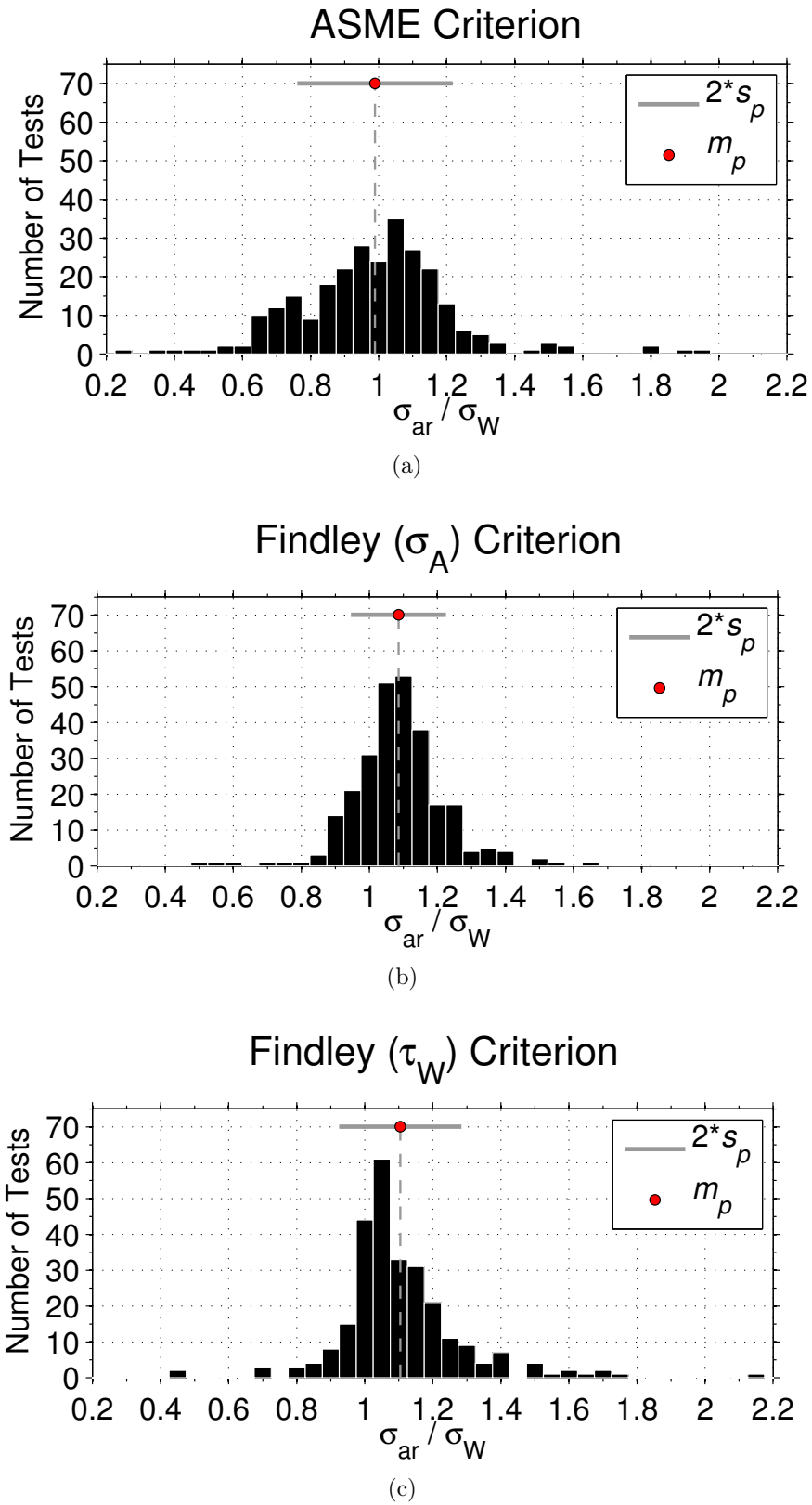


Figure 5.3.2.: Histograms of all predictions from the ASME criterion and Findley $k(\sigma_A)$ and $k(\tau_W)$ for 268 tests.

5. Results

From figure 5.3.1 and 5.3.2, it is apparent that outliers are present. For the normal stress criterion, the outliers on the conservative side are caused by the aluminium alloy 76S-T61, test nr 227 and 235. Large mean stresses for σ_x are present in both tests. Compared to the other criteria, the predictions are closely gathered on the non-conservative side.

Some test-series seem to be the cause of outliers for many criteria, namely 34CrMo4 V. This test-series yields outliers for Mises-Sines, Tresca-Sines, ASME and both variations of Findley. Test nr 212 with $\tau_{xym} = 794.6$ MPa causes the most non-conservative prediction for both Sines-criteria and the ASME-criterion. Tresca-Sines and the ASME-criterion produce low quality predictions for cast iron from Nishihara/Kawamoto, and these cause the conservative outliers seen in the histograms.

5.3.2. Comparison of Predictions for Material Groups

The materials were grouped into three distinct material divisions: carbon and low alloy steels, aluminium alloys and cast irons. A summary of the predictions are given in table 3.1. The group with carbon and low alloy steels is by far the largest, consisting of 221 experiments ($\approx 82.5\%$ of all tests).

The normal stress criterion yields non-conservative predictions for all material groups, but more for the carbon/low alloy steels and aluminium 76S-T61. An acceptable degree of accuracy is noticeable for the predictions regarding cast irons. The traditional assessment method and the ASME-assessment method provide no differences in predictions.

Mises-Sines and Mises-Sines-ASME yield quite similar predictions, with a mean value closer to one for the latter. A high degree of spread is observed for cast irons.

Tresca-Sines provide a quite large spread in predictions for all three material groups, and the mean-value is closer to 1 for the carbon/low alloy steels than aluminium and cast irons.

The ASME-criterion predictions have a slightly non-conservative mean value for carbon and low alloy steels, but a large spread. For both the aluminium tests and cast irons, the mean value is conservative. Predictions for cast iron are marked by high spread and are thus inaccurate.

The Findley criterion shows an improvement in mean value for carbon and low alloy steels, and cast irons, when assessed with the ASME-method. This is especially pronounced for Findley (σ_A) and carbon/low alloy steels. Predictions made with Findley (τ_W)-ASME are better but still contains a high degree of spread.

Table 5.2.: Comparison of predictions for all criteria and different loading cases. The predictions are presented as the mean value plus/minus one standard deviation, $m_p \pm s_p$.

Assessment Method	Criterion					
	Normal Stress	Mises-Sines	Tresca-Sines	ASME	Findley (σ_A)	Findley (τ_W)
<i>All 268 tests regardless of stress ratio or stress components.</i>						
Prop. method	0.88 ± 0.14	1.04 ± 0.15	1.08 ± 0.22	-	1.09 ± 0.14	1.10 ± 0.18
ASME-method	0.88 ± 0.14	1.02 ± 0.16	1.09 ± 0.21	0.99 ± 0.23	1.02 ± 0.15	1.03 ± 0.17
<i>Pure shear, $R=-1$, 11 tests in total.</i>						
Prop. method	0.69 ± 0.14	1.20 ± 0.24	1.38 ± 0.28	-	1.12 ± 0.21	1.03 ± 0.04
ASME-method	0.69 ± 0.14	1.20 ± 0.24	1.38 ± 0.28	1.38 ± 0.28	1.12 ± 0.21	1.03 ± 0.04
<i>One normal stress and one shear component present, $R=-1$, $\alpha_{xy} = 0^\circ$, 48 tests in total.</i>						
Prop. method	0.93 ± 0.08	1.06 ± 0.08	1.14 ± 0.12	-	1.06 ± 0.08	1.04 ± 0.03
ASME-method	0.93 ± 0.08	1.06 ± 0.08	1.14 ± 0.11	1.14 ± 0.12	1.06 ± 0.08	1.04 ± 0.03
<i>One normal stress and one shear component present, $R=-1$, $\alpha_{xy} \neq 0^\circ$, 33 tests in total.</i>						
Prop. Meth	0.81 ± 0.12	1.09 ± 0.14	1.00 ± 0.20	-	1.03 ± 0.13	1.02 ± 0.08
ASME-method	0.81 ± 0.12	0.93 ± 0.16	1.02 ± 0.20	1.00 ± 0.20	0.94 ± 0.13	0.92 ± 0.11
<i>One normal stress and one shear component present, $R \neq -1$, $\alpha_{xy} = 0^\circ$, 26 tests in total.</i>						
Prop. method	0.95 ± 0.19	1.01 ± 0.19	1.07 ± 0.21	-	1.16 ± 0.13	1.23 ± 0.24
ASME-method	0.95 ± 0.19	1.01 ± 0.19	1.07 ± 0.21	0.89 ± 0.19	1.04 ± 0.16	1.10 ± 0.20

Table 5.3.: Comparison of predictions for all criteria, a selection of stress components present, and different groups of materials. No selection of stress-ratios or the like have been made. The predictions are presented as the mean value plus/minus one standard deviation, $m_p \pm s_p$.

Assessment Method	Criterion					
	Normal Stress	Mises-Sines	Tresca-Sines	ASME	Findley (σ_A)	Findley (τ_w)
<i>Two normal and one shear stress component regardless of stress ratio and phase shift, 18 tests in total.</i>						
Prop. method	0.84 \pm 0.12	1.01 \pm 0.08	1.10 \pm 0.21	-	1.07 \pm 0.14	1.18 \pm 0.18
ASME-method	0.84 \pm 0.12	1.06 \pm 0.15	1.11 \pm 0.21	0.86 \pm 0.21	1.01 \pm 0.14	1.10 \pm 0.16
<i>Two normal stress components regardless of stress ratio and phase shift, 19 tests in total.</i>						
Prop. method	0.83 \pm 0.10	0.91 \pm 0.14	0.96 \pm 0.35	-	0.92 \pm 0.21	0.92 \pm 0.22
ASME-method	0.83 \pm 0.10	1.04 \pm 0.12	1.02 \pm 0.27	0.81 \pm 0.14	0.89 \pm 0.19	0.88 \pm 0.20
<i>Carbon- and low alloy steels, 221 tests in total, nr. 1-221.</i>						
Prop. method	0.86 \pm 0.14	1.03 \pm 0.12	1.07 \pm 0.20	-	1.08 \pm 0.13	1.10 \pm 0.18
ASME-method	0.86 \pm 0.14	1.01 \pm 0.13	1.08 \pm 0.19	0.97 \pm 0.20	1.01 \pm 0.15	1.03 \pm 0.17
<i>Aluminium 76S-T61, 21 tests in total, nr. 222-242.</i>						
Prop. method	0.92 \pm 0.19	1.06 \pm 0.11	1.14 \pm 0.13	-	1.02 \pm 0.13	1.03 \pm 0.08
ASME-method	0.92 \pm 0.19	1.06 \pm 0.11	1.14 \pm 0.13	1.07 \pm 0.14	1.02 \pm 0.13	1.03 \pm 0.08
<i>Cast Irons, 26 tests in total, nr. 243-268.</i>						
Prop. method	0.97 \pm 0.08	1.07 \pm 0.33	1.11 \pm 0.40	-	1.19 \pm 0.18	1.17 \pm 0.21
ASME-method	0.97 \pm 0.08	1.04 \pm 0.32	1.11 \pm 0.40	1.09 \pm 0.40	1.06 \pm 0.21	1.11 \pm 0.15

5.4. Stress-Cycle of Dynamically Loaded Component

The results of the fatigue assessment for the dynamically loaded component with stresses plotted in figure 4.10.1 are given in table 5.5. All stress-values are normalized with respect to $|\sigma_x|_{\max}$. The stress cycle was evaluated using all criteria and both assessment methods.

The conversion given in equation 5.1 gives the equivalent uniaxial amplitude normalized with respect to σ_W . Values for the stress cycle normalized on σ_W are given in table x.

$$\frac{\sigma_{ar}}{\sigma_W} = \frac{\sigma_{ar}}{|\sigma_x|_{\max}} \cdot \frac{|\sigma_x|_{\max}}{\sigma_W} \quad (5.1)$$

All predictions $\frac{\sigma_{ar}}{|\sigma_x|_{\max}}$ are below 1, and so with the assumption that $|\sigma_x|_{\max} < \sigma_W$ for the real material (not the approximated $\sigma_W = 450$ MPa), failure is not predicted.

For the normal stress criterion, the proportional assessment method and ASME-method yield no differences in predictions. The critical plane is unchanged between the two, and the stresses which result in the largest $\frac{\sigma_{ar}}{|\sigma_x|_{\max}}$ occur on the same steps. It is noticeable that the critical plane is “chosen” based on the highest combination of normal stresses, as the shear stress occurring on the same plane and the resulting shear stress amplitude is lower than those for the shear stress criteria.

For the Mises-Sines criterion, the variation Mises-Sines-ASME yield a more conservative value, but the stress values σ_{ij} used in the assessment of the criteria are all taken from the same steps.

The Tresca-Sines and Tresca-Sines-Mises criterion show differences in the critical plane, as well as a marginal difference in $\frac{\sigma_{ar}}{|\sigma_x|_{\max}}$. The values however are taken from the same steps. The ASME-criterion yields the same $\frac{\sigma_{ar}}{|\sigma_x|_{\max}}$ as Tresca-Sines-ASME. Both criteria regardless of assessment method (for Sines-Mises criterion) yield the most non-conservative predictions out of all the fatigue criteria.

The Findley criterion for both $k(\sigma_A)$ and $k(\tau_W)$ yield identical results, but marginally different critical planes.

Figure 5.4.1 show the stresses on the predicted critical planes for the normal stress criterion, Tresca-Sines and the Findley (σ_A) criterion throughout the cycle. For the normal stress criterion, the plane is chosen based on the normal mean and amplitude stress. This is visible in 5.4.1 (a). The Findley (σ_A) criterion finds the critical plane based on shear stress amplitude and maximum occurring normal stress. Compared to

5. Results

Table 5.4.: Results of stress-cycle assessment for all criteria and both assessment methods normalized with σ_W .

	Normal Stress	Mises-Sines	Tresca-Sines	ASME	Fin. (σ_A)	Fin. (τ_W)
<i>Proportional assessment method</i>						
$\frac{\sigma_{ar}}{\sigma_W}$	0.44	0.43	0.33	-	0.41	0.39
<i>ASME-method</i>						
$\frac{\sigma_{ar}}{\sigma_W}$	0.44	0.40	0.33	0.33	0.41	0.39

the critical plane predicted by the normal stress criterion, the variation in parameters taken into account for each criterion becomes apparent.

Figure 5.4.1 also show at which step the extreme values of stresses on the different critical planes occur. This coincides well with the steps given in table 5.5.

5.4. Stress-Cycle of Dynamically Loaded Component

Table 5.5.: Results of stress-cycle assessment for all criteria and both assessment methods. The names for the criteria are shortened, so that NS corresponds to the normal stress criterion etc.

		NS	MS	TS	ASME	F (σ_A)	F (τ_W)
<i>Proportional assessment method</i>							
$\frac{\sigma_{ar}}{ \sigma_x _{max}}$		0.97	0.96	0.73	-	0.90	0.86
ϕ ($^\circ$)		6	-	56	-	150	149
$\frac{\sigma_{max}(\phi)}{ \sigma_x _{max}}$	Value	0.91	-	(0.38)	-	0.87	0.86
	Step	23	-	23		23	23
$\frac{\sigma_{min}(\phi)}{ \sigma_x _{max}}$	Value	-1.07	-	(-0.86)	-	(-0.49)	(-0.48)
	Step	89		89		89	89
$\frac{\tau_{max}(\phi)}{ \sigma_x _{max}}$	Value	(0.10)	-	0.47	-	0.23	0.24
	Step	54		89		23	23
$\frac{\tau_{min}(\phi)}{ \sigma_x _{max}}$	Value	(-0.30)	-	-0.27	-	-0.50	-0.49
	Step	76		23		89	89
<i>ASME-method</i>							
$\frac{\sigma_{ar}}{ \sigma_x _{max}}$		0.97	0.89	0.74	0.74	0.90	0.86
ϕ ($^\circ$)		6	-	146	-	150	149
Interval		23-89	23-89	23-89	23-89	23-89	23-89

() Stress values in paranthesis not used by the criterion.

5. Results

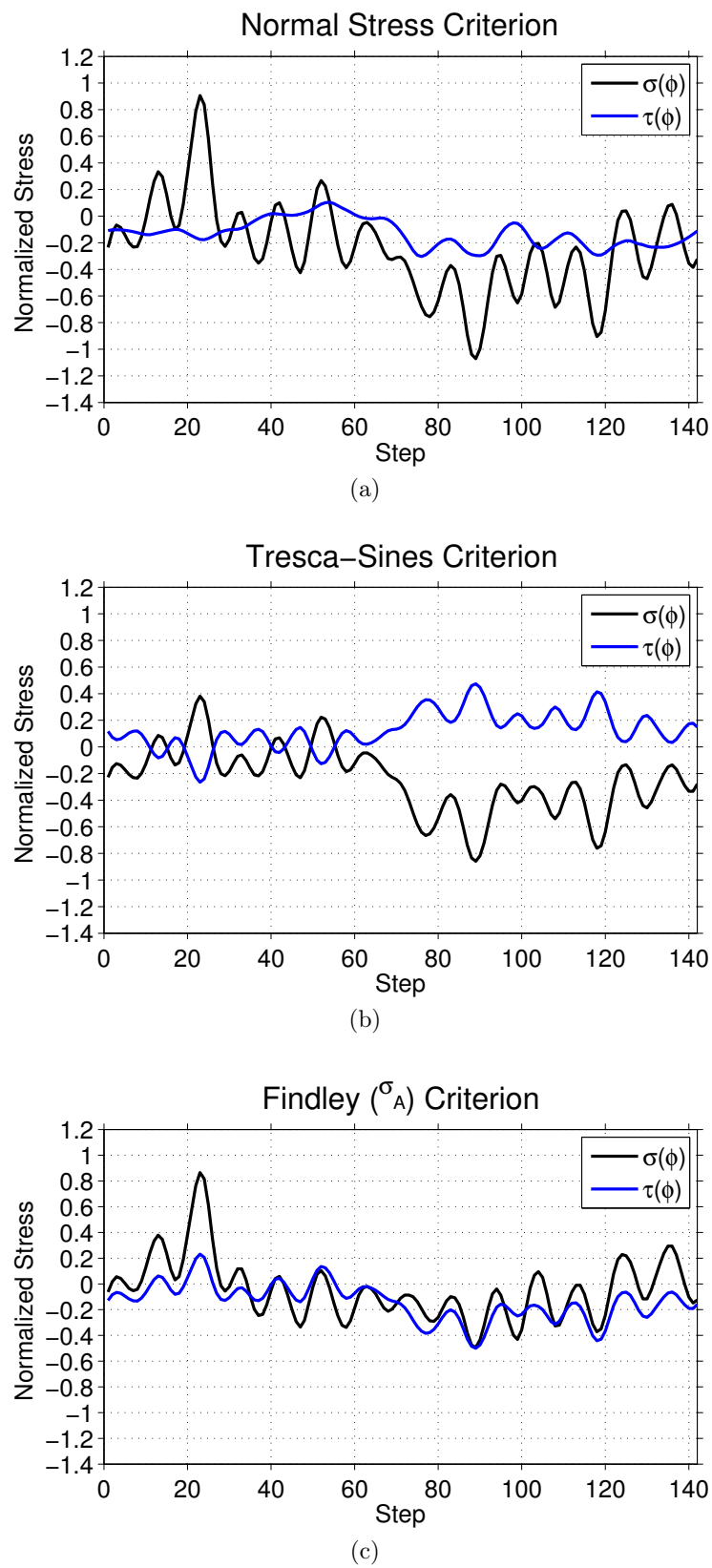


Figure 5.4.1.: Stresses throughout the cycle on critical planes predicted by the critical-plane criteria.

6. Discussion

6.1. Requirements of a Fatigue Criterion

The fatigue criteria are reviewed based on three requirements. In search for the perfect fatigue criterion, these requirements should all be fulfilled.

1. Accuracy of predictions
2. Criterion should be based on physical properties proven to have an effect on fatigue damage mechanisms
3. Ease of use and implementation of criterion

A *good* criterion should produce accurate predictions for a wide selection of materials and loading cases. Parameters such as angular frequency, phase shift and R -ratios should all be correctly accounted for. The normalized fatigue prediction parameters $\frac{\sigma_a}{\sigma_w}$ given in table 5.2 and 5.3 are a quantitative measure of the accuracy of each criterion.

The criteria are assessed based on their usability and ease of implementation. The practicing engineer is taken into account on this point. If the criterion is difficult to utilize, its general accept in the engineering community will probably suffer as a result.

Every criterion should as well be based on logical and proven material dependencies. As cumulative fatigue damage is a process involving many variables, such parameters should be taken into account as are proven to have an effect on fatigue life.

Hence, a perfect criterion is one which is based on proven and logical material dependencies, which gives excellent predictions, and is simple to use and implement. In reality, these three requirements might be extremely difficult to fulfil. They do however provide a platform on which to compare and evaluate each criterion. The last two requirements might suffer from subjective opinions. With the increased availability of fatigue post-processors, the second requirement can be questioned. The literature commonly focus on accuracy of predictions, without thought to practicing

6. Discussion

engineers. A trade-off between these three requirements is generally the criterion which will see the most widespread use.

6.2. Assessment and Suitability of Criteria

An accurate prediction is as previously stated when the equivalent uniaxial stress amplitude σ_{ar} coincides with the uniaxial fully reversed fatigue limit σ_W . As a certain degree of scatter is expected in fatigue tests, the overall, mean value of predictions serve as a quantitative measure of the predictability of a criterion. The predictability is presented as the mean value of predictions plus/minus the sample standard deviation, $m_p \pm s_p$. A high degree of accuracy is then characterized by m_p close to one, and s_p close to zero. It is important that the two are compared together. One might argue that a low spread is preferable to a perfect mean value equal to 1, as the mean value can be countered by introducing a fitting safety factor.

6.2.1. Normal Stress Criterion

The normal stress criterion show overall inaccurate and non-conservative predictions for materials, where failure is expected to occur based on shear-stress induced fatigue cracks. The results for brittle materials with a $\frac{\tau_W}{\sigma_W}$ -ratio close to 1 are however significantly better, and the predictions are far better than the shear-stress criteria. The physical relevance of the criterion is well established for uniaxial, proportional cases as it is based on the Hempel-Morrow line.

Out of the critical-plane criteria, the normal stress criterion is by far the easiest to use when utilizing the proportional assessment method. This is due to the material parameters needed for the fatigue assessment only being the mean stress sensitivity M and the fatigue limit σ_W . In addition, only the normal-stress on the critical plane is taken into account, making calculations easier. When combined with the ASME-method, no differences in predictability were found. This is possibly due to the fact that only the normal stress component on the plane is taken into account, but this is further discussed in section 6.3. The computational difficulty is however increased whenever the ASME-method is used, and since no differences in predictability were found for the normal stress criterion, this should be taken into account when using the criterion.

6.2.2. Mises-Sines Criterion

The Mises-Sines criterion yields good predictions for proportional cases when assessed with the proportional-method. For shear-dominated cases however, the criterion might be expected to yield inaccurate predictions. The validity of stress invariants may be questioned for stress histories of a non-proportional nature, but comparing the predictions for both the proportional-method and the ASME-method show that they are fairly close to each other. The predictions yielded when using the latter method are only slightly better for Mises-Sines-ASME, but the *decrease* in computability is distinct. Still, the mean value of predictions for Mises-Sines-ASME is very accurate, on par with the Findley criterion. Since it is based on stress-invariants rather than critical-plane methodology, the implementation of Mises-Sines is fairly simple. The criterion is also based on empirical data for proportional loading.

6.2.3. Tresca-Sines Criterion

The Tresca-Sines criterion is, together with the normal stress criterion, fairly simple to use. The critical-plane is relatively easy to determine, since it is determined by the maximum shear stress amplitude. Utilizing the stress-invariant for mean stresses, the fatigue assessment as a whole is relatively simple. The predictions however, are marked by a high degree of spread, especially for brittle materials such as cast irons. The predictions for Tresca-Sines-ASME are somewhat similar overall, and thus the ASME-method only contributes negatively in terms of computationability.

6.2.4. ASME-Criterion

The ASME-criterion, while not modified for mean stresses yield (not surprisingly) inaccurate predictions with a high degree of spread. The good mean value of X for all of the 268 fatigue tests is a result of pure chance, as the more differentiated stress cases show. For stresses with ratio $R = -1$, the predictions are equal to the Tresca-Sines criterion. This gives grounds to the validity of the approximation $\sigma_{\text{eq,T,a}} \approx 2\tau_{\text{a,max}}(ASME)$. The criterion itself is somewhat easier to compute than the critical-plane criteria, not requiring to calculate stresses on every plane $\phi \in [0^\circ, 180^\circ]$, and provided the extreme-values and their points in time are known. When these points in time are *unknown*, the computability decreases.

6.2.5. Findley Criterion

The Findley criterion is the most extensive criterion to compute and implement. It requires the determination of k , here only shown for pure shear or pure normal stresses and the stress ratios $R = -1$ and $R = 0$ in equation (2.28). Since the fatigue limits used to determine k yield different values, the notion of k as a *constant* should be addressed. Since the k have such a large impact on the accuracy of predictions, the uncertainty of which two fatigue limits should be combined increases insecurity around the implementation. In this thesis, two k 's were evaluated with σ_W in combination with σ_A and τ_W . From table 5.2 the difference in predictions for $k(\sigma_A)$ and $k(\tau_W)$ are apparent. Overall, the predictions when $k(\sigma_A)$ is used are more accurate, with a mean value closer to 1 and slightly lesser spread than for $k(\tau_W)$. For fully reversed, pure shear stresses the predictions with $k(\tau_W)$ are considerably better than the $k(\sigma_A)$. This might indicate that for stress cycles dominated by shear-stresses, k should be determined using the shear fatigue limit τ_W , and the opposite is valid for cycles where normal-stresses dominate.

As a critical-plane criterion, it makes use of both the shear and normal-stress on the critical plane. This makes the calculation slightly more challenging than the other critical plane criteria reviewed here, as they all only utilize one stress component (either the shear stress or normal stress). The effect is however diminishing when using computational resources like MATLAB. A significant improvement of the mean value of predictions is observed when using the ASME-method, although the usability of the criterion is diminished. Not only are the stresses for each stress component on the plane assessed together with the stresses at every other point in time calculated, but this has to be done for $\phi \in [0^\circ, 180^\circ]$.

6.3. Proportional Method vs ASME-Method

Fatigue criteria derived for proportional loading are commonly used to assess situations where the loading is non-proportional. The common method of determining stress parameters and subsequently the criteria, is here called the *proportional-method* and explained in section 4.5.

According to the proportional method, global extreme values should be used to determine relevant stress components used by the fatigue criterion. The alternating and mean stress components may then be found by equation (2.10) and (2.11). For non-proportional loading however, the stress-values utilized by a criterion may occur at potentially large differences in time. An example of such a stress cycle

6.3. Proportional Method vs ASME-Method

is presented in figure 6.3.1, and the question can be raised of the validity of the proportional method for such cases.

Assuming that the plane on which the stresses in figure 6.3.1 are working, is the *critical plane* for both the normal stress criterion and the Findley criterion. This assumption is only done here to explain the advantages of the ASME-method.

The proportional method of determining stress values, will yield the maximum shear stress amplitude on the plane as $\tau_a(\phi) = \frac{1}{2}[\tau(\phi, t_1) - \tau(\phi, t_1)]$. The shear stresses occurring at the points in time t_1 and t_2 are used. The normal stress amplitude may be determined as $\sigma_a(\phi) = \frac{1}{2}[\sigma(\phi, t_3) - \sigma(\phi, t_1)] = \frac{1}{2}[\sigma(\phi, t_3) - \sigma(\phi, t_2)]$, as the normal stress occurring at t_1 and t_2 are equal. The mean stress components are determined accordingly.

The normal stress criterion makes use of both $\sigma_a(\phi)$ and $\sigma_m(\phi)$, while the shear stress components on the plane are disregarded. The normal stresses occurring in the relative vicinity of t_3 then govern the predictions made by the criterion. The Findley criterion utilizes both $\tau_a(\phi)$ and $\sigma_{\max}(\phi)$, and while the largest $\tau_a(\phi)$ is found around t_1 and t_2 , the maximum normal stress occurs at t_3 . Since $t_3 \gg t_1, t_2$ it is not obvious how the normal stress may have a direct, physical influence on the fatigue damage. This aspect is however neglected when using the proportional method. The determined stress-values are used indiscriminately, only in capacity of occurring on the same plane *throughout* the cycle.

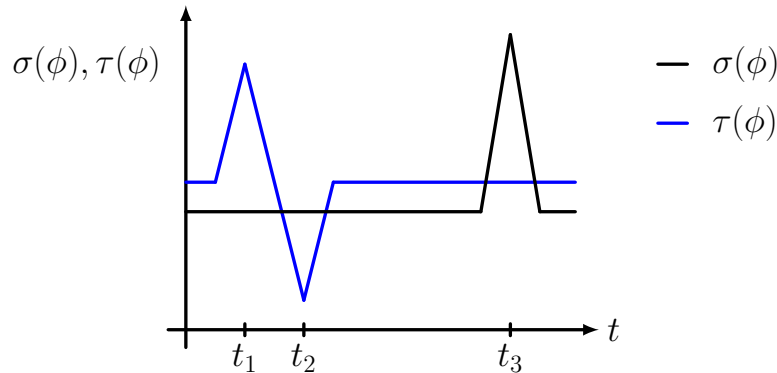


Figure 6.3.1.: Stress cycle with one shear and one normal stress component.

The proposed ASME-method attempts to remedy this by using stress-components calculated on intervals between two points in time, where the stresses are hypothesized to have a specific relevance to each other. Stress components for an interval $[\hat{t}, t]$ are then based only on the stresses occurring at time \hat{t} and t . When following the ASME-method, each stress component at each point in time, is compared relative to every other stress component, occurring at every other point in time. The

6. Discussion

maximum and minimum values on each interval are used to find amplitudes and mean stresses, and so each fatigue criterion may be calculated interval-wise. The interval in time which corresponds to the largest predicted σ_{ar} then governs fatigue damage on the plane.

For the cyclic stresses in figure 6.3.1, the intervals $[t_1, t_3]$ and $[t_2, t_3]$ yield the same amplitude and mean normal stress. When using the ASME-method, the normal stress criterion then predicts the same local σ_{ar} for both intervals. For interval $[t_1, t_2]$, the amplitude $\sigma_a(\phi) = 0$, which will yield a smaller σ_{ar} only based on $\sigma_m(\phi)$.

For the Findley criterion in combination with the ASME-method, the interval $[t_1, t_2]$ yields the largest shear stress amplitude, but a $\sigma_{\text{max}}(\phi) = \sigma(\phi, t_1) = \sigma(\phi, t_2)$. The interval $[t_1, t_3]$ yields a smaller shear stress amplitude, but a significantly larger maximum normal stress. The interval $[t_2, t_3]$ yields the same values as for $[t_1, t_3]$, with exception of a negative $\tau_m(\phi)$. The mean shear stress is however not taken into account by the Findley criterion.

The influence of this assessment method is larger for the Findley criterion, and in a positive way (see section 5.3). This might be caused by the fact that both normal- and shear stresses are taken into account. For the normal stress criterion however, the ASME-method were in this case reduced to a laborious alternative for determining the amplitude and mean normal stress. The ASME-method then shows promise, and deserves further testing. This is especially for critical-plane criteria where both normal- and shear stresses are taken into account.

6.4. Fatigue Assessment of Stress Cycle

An interesting aspect when comparing the results from the fatigue database with the results for the stress cycle, is the relative differences between the criteria predictions. Based on the trend from the fatigue tests as shown in the failure assessment diagrams, the normal stress criterion should yield a more non-conservative prediction than the other criteria for most combinations of shear and normal stresses. In that respect, the $\frac{\sigma_{\text{ar}}}{\sigma_{\text{W}}}$ predicted by the normal stress criterion should be below the $\frac{\sigma_{\text{ar}}}{\sigma_{\text{W}}}$ -values for the criteria based on shear stress. It is however above these values, which is intriguing. The summaries are mainly done for combinations of one normal stress together with a shear stress, and do not provide sufficient information on cases where two normal stresses are present. The low value of ϕ_{crit} also show that the critical plane is quite close to the x-axis, which indicates that the fatigue assessment is dominated by the quite large $\frac{\sigma_x}{|\sigma_x|_{\text{max}}}$ -component. Assuming the fatigue assessment

6.5. A Note on the Availability of Fatigue Test-Data

is dominated by the $\frac{\sigma_x}{|\sigma_x|_{\max}}$ -component, which might be a more than reasonable assumption, this would correspond to the bottom right corner of a fatigue assessment diagram. The overall similarity of the the $\frac{\sigma_{ax}}{\sigma_w}$ -values support this.

The ASME-criterion however stands out as the most non-conservative. Since it does not take mean stresses into account, this is reasonable, as the other criteria account for mean stresses and are expected to yield predictions closer to failure on the conservative side.

6.5. A Note on the Availability of Fatigue Test-Data

This thesis builds on a now long tradition of comparing multiaxial fatigue criteria with tests found in the literature. In this regard it falls in line with several works based on the same basic pattern. Older criteria are compared with a newly proposed criterion or assessment method, using limited test data collected from the literature, often from unreliable sources. It is clear that the topic of fatigue test data for proportional and non-proportional data deserves to be discussed further.

As table 4.1 shows, an extensive search after usable and trustworthy experimental results was conducted. Gathering such experimental data proved to be a long, and often frustrating process, during which several concerns was discovered.

The availability of readily usable fatigue test results is a major issue. Countless experiments have been performed, but several authors only publish the results and are content with referring to the test data used. In the rare case that the test data are presented, it is often in the form of graphs that require a potential inaccurate reading in order to become usable. Several citations are also lacking in accuracy, as they occasionally hail non-primary sources as the origin of the data.

With the apparent demand of usable experimental data, researchers are forced to carry out own investigations or make do with tests provided in the literature. As so few new experiments are published, most of the available data stem from relatively old sources. The test series performed by Nishihara & Kawamoto [27], Lempp [38], Zenner et al. [35, 33] and Froustey & Lasserre [24] are among the most frequently cited. This in itself is problematic for a number of reasons. The Nishihara & Kawamoto data were published in Japan in 1945. The original Japanese paper is extremely hard to procure, as well as any translated versions. The amount if use seems in no way to be affected by the elusiveness of the original publication. With no copy of the original source available, great caution should be exercised with respect

6. Discussion

to the quality and aptitude of these investigations. Information on how the tests were conducted is lost, assumptions are unknown, testing apparatus is uncertain and so on. This leaves the user to trust in secondary sources at best when searching for data suitable for validating purposes.

Of the roughly 30 papers reviewed in connection with this thesis, the Nishihara & Kawamoto data is referred to in 12 of them. It is questionable as well that such a large amount of later investigations are relying on experiments from the same source. New and proposed criteria are constantly being tried against the same experiments. The lack of new input can have a severe impact if this trend continues. This thesis is no exception, as all the examples mentioned are included and used here. This is the result of a trade-off between need and resources. The need and wish for as many tests as possible to be able to provide an in-depth statistical evaluation of predictions, against the urge to only employ safe original sources and up to date experiments.

Several private databases containing fatigue experiments are known to exist, and are used to great effect by their assemblers. Most notably are the databases by Papuga and Susmel [44]. In an attempt to remedy this, Papuga has amassed a large amount of fatigue tests from the literature on his webpage [5]. These data are available to the public, and provide an excellent starting point for further investigations.

One can only speculate on the reasons why so few new experiments are being published. Since up to date experimental data are so scarce, new and fresh experimental data would surely receive a lot of attention.

6.6. Continued Work and Suggested Improvements

When comparing the work done in this thesis with the quite extensive problem description, it becomes apparent that only a portion is covered here. In addition to explore the topics not included here, some ideas for further investigation also emerged as a result of the investigation.

Expansion of the fatigue database Due to the lack of test data, it would be desirable to perform in-house fatigue testing of select materials. Not only would they serve as a trustworthy platform for future investigations, but would surely attract the attention to any papers they are published in. A further expansion of the existing test-database with experimental data from the literature should be

6.6. Continued Work and Suggested Improvements

considered as well. Especially the sections regarding aluminium alloys and cast irons should be improved in order to give statistically sufficient results.

More criteria combined with the ASME-method A total of 11 different versions of well-known fatigue criteria were examined during this investigation. The Findley-ASME criterion stands out, with an overall increase in accuracy compared to the traditional Findley criterion. The ASME-method of assessing stress cycles shows promise and deserves to be further tested on other criteria.

Improved calculation scripts and database management systems All of the main calculations in this thesis were done in MATLAB, while the literature tests were gathered and stored in Excel. They were chosen at the time out of practicality and previous experience. While the MATLAB-Excel setup performed suitably well, there is some room for improvement. The storing of data in Excel works fine for a limited amount of data. As the amount increases, management of the data becomes increasingly hard to handle. Large Excel-sheets are also prone to accidental misentries, where faulty values may go unnoticed.

The scripts used to perform the fatigue assessment were all made by the author. In no way should they be considered as optimal in terms of computational elegance and optimization. This should not have an effect on the results, but will provide scripts that run smoother. In that regard, input should be sought from someone with extended computational experience. Other programming-languages such as Python should also be considered. As the fatigue database is expanded, other options for storing the data should be considered. Available possibilities are dedicated database management systems such as MySQL.

7. Conclusion

The main purpose of this thesis was to provide a critical review of the fatigue assessment of components subjected to non-proportional stress histories. A large database consisting of 268 biaxial fatigue limits for combined loading, spanning 27 test series and 20 materials was assembled. For the sake of comparison, cases for both proportional and non-proportional loading were included.

Gathering experimental data from credible sources proved to be an exhausting process. Several comprehensive databases of the sort are known to exist, but are not, with the exception of occasionally republished snippets, readily available to the fatigue community at large. As a result, engineers and scientists are forced to make the best out of old experiments from sources of often uncertain quality. A total of 268 experimental tests were gathered in this thesis in an attempt to remedy this, which in this context can be seen as formidable. The experimental data, some of it very old, are still commonly used for validating purposes. With this in mind they have been reproduced here.

The experimental data was evaluated using five criteria intended for multiaxial fatigue assessment. The original criteria included in the assessment were the normal stress criterion, Sines criterion with the von Mises stress amplitude, Sines criterion with the Tresca stress amplitude, the ASME-criterion and the Findley criterion. In addition to the traditional, *proportional-method* based on max-min stress-values over the course of a cycle, an *ASME-method* is proposed and implemented. The ASME-method calculates stress-values based on *intervals*, which may or not coincide with the proportional-method of assessing stresses throughout a cycle. Both the criteria and the two assessment-methods were evaluated and compared with respect to usability and quality of predictions.

The normal stress criterion yielded non-conservative predictions for both the carbon/low alloyed steels and the aluminium alloy 76S-T61 included in the compiled fatigue database. The accuracy for brittle materials was however unprecedented. The ASME-criterion without correction for mean stresses yielded an almost astonishing overall mean predicted value of 0.99. The standard deviation however was the highest for all criteria, indicating a high spread in predictions. These were chiefly

7. Conclusion

caused by test data with nonzero mean stresses. For the Findley criterion evaluated with two different values of k , the ASME-assessment method yielded a *significant improvement* in the quality of predictions. However, the ASME-method had no effect on other criteria such as the normal stress criterion. This indicates that the ASME-method may have a positive effect on other criteria, and deserves further evaluation.

From a user-friendly point of view, the Mises-Sines criterion based on stress invariants is the least challenging. Even though the concept of the von-Mises stress invariant is not valid for non-proportional loading, the criterion yielded relatively good predictions overall. The critical plane criteria, here represented by normal stress, Tresca-Sines and Findley all require computations to be done over a wide range of angles. Findley requiring the determination of at least the material parameter k is the least user friendly of the three. The computability is severely decreased when the criteria are assessed with the ASME-method. This is especially the case for critical-plane criteria. With the overall result of improved predictions, this is an aspect that needs to be considered.

The overall conclusion of this thesis is that multiaxial fatigue assessment is an incredibly complex process. Knowledge in a variety of disciplines is necessary in order to effectively perform a proper evaluation, and computational experience is a must. The benefit of performing such an analysis is the better predictability of fatigue failure.

Bibliography

- [1] J. A. Schmidt. The definition of structural engineering. <http://www.structuremag.org/article.aspx?articleID=829>, last checked: 13/12- 2013.
- [2] I. V. Papadopoulos, P. Davoli, C. Gorla, M. Filippini, and A. Bernasconi. A comparative study of multiaxial high-cycle fatigue criteria for metals. *International Journal of Fatigue*, 19(3):219–235, 1997.
- [3] A. Carpinteri and A. Spagnoli. Multiaxial high-cycle fatigue criterion for hard metals. *International Journal of Fatigue*, 23(2):135 – 145, 2001.
- [4] J. O. Nøkleby. *Fatigue under multiaxial stress conditions*. PhD thesis, Division of Machine Elements, The Norwegian Institute of Technology, Trondheim, Norway., 1980.
- [5] J. Papuga. Pragtic website. <http://www.pragtic.com/>, last checked: 13/12-2013.
- [6] A. Troost, O. Akin, and F. Klubberg. Versuchs-und rechenaten zur dauerschwingfestigkeit von metallischen werkstoffen unter mehrachsiger beanspruchung. *Materialwissenschaft und Werkstofftechnik*, 23(1):1–12, 1992.
- [7] N. E. Dowling. *Mechanical behavior of materials: engineering methods for deformation, fracture, and fatigue*. Pearson, Boston, 4th ed edition, 2013.
- [8] D. F. Socie and G. B. Marquis. *Multiaxial fatigue*. Society of Automotive Engineers, Warrendale, Pa., 2000.
- [9] G. Härkegård. Fatigue assessment of engineering components subjected to arbitrary multiaxial stress histories, February 2013.
- [10] G. Sines, J. L. Waisman, and T. J. Dolan. *Metal fatigue*, pages 145–169. McGraw-Hill, 1959.
- [11] E. Roos. *Festigkeitslehre 1*. Institut für Materialprüfung, Werkstoffkunde und Festigkeitslehre, Universität Stuttgart, 34. auflage edition, 2010.

Bibliography

- [12] W. N. Findley. *A theory for the effect of mean stress on fatigue of metals under combined torsion and axial load or bending*. Basic research on fatigue failures under combined stress: Technical report. Engineering Materials Research Laboratory, Division of Engineering, Brown University, 1958.
- [13] B. Crossland. Effect of large hydrostatic pressures on the torsional fatigue strength of an alloy steel. In *Proc. Int. Conf. on Fatigue of Metals, Institution of Mechanical Engineers, London*, pages 138–149, 1956.
- [14] DL. McDiarmid. A shear stress based critical-plane criterion of multiaxial fatigue failure for design and life prediction. *Fatigue & Fracture of Engineering Materials & Structures*, 17(12):1475–1484, 1994.
- [15] DL. McDiarmid. A general criterion for high cycle multiaxial fatigue failure. *Fatigue & Fracture of Engineering Materials & Structures*, 14(4):429–453, 1991.
- [16] T. Matake. An explanation on fatigue limit under combined stress. *Bulletin of JSME*, 20(141):257–263, 1977.
- [17] W. Navidi. *Statistics for Engineers and Scientists*, pages 13–14. McGraw-Hill, second edition.
- [18] *Rechnerischer Festigkeitsnachweis für Maschinenbauteile*, page 87. VDMA-Verlag, 6 edition, 2012.
- [19] *Rechnerischer Festigkeitsnachweis für Maschinenbauteile*, pages 96–97. VDMA-Verlag, 6 edition, 2012.
- [20] H. J. Gough and H. V. Pollard. The strength of metals under combined alternating stresses. *Proceedings of the Institution of Mechanical Engineers*, 131(1):3–103, 1935.
- [21] S. Lasserre and C. Froustey. Multiaxial fatigue of steel - testing out of phase and in blocks: validity and applicability of some criteria. *International journal of fatigue*, 14(2):113–120, 1992.
- [22] H. Zenner, R. Heidenreich, and I. Richter. Dauerschwingfestigkeit bei nichtsynchrone mehrachsiger beanspruchung. *Materialwissenschaft und Werkstofftechnik*, 16(3):101–112, 1985.
- [23] A. Banvillet, T. Palin-Luc, and S. Lasserre. A volumetric energy based high cycle multiaxial fatigue criterion. *International journal of fatigue*, 25(8):755–769, 2003.
- [24] C. Froustey and S. Lasserre. Multiaxial fatigue endurance of 30ncd16 steel. *International Journal of Fatigue*, 11(3):169 – 175, 1989.

- [25] H. J. Gough. Engineering steels under combined cyclic and static stresses. *Proceedings of the Institution of Mechanical Engineers*, 160(1):417–440, 1949.
- [26] W. N. Findley. Combined-stress fatigue strength of 76s-t61 aluminum alloy with superimposed mean stresses and corrections for yielding, 1953.
- [27] T. Nishihara and M. Kawamoto. The strength of metals under combined alternating bending and torsion with phase difference. *Memories of the College of Engineering, Kyoto Imperial University*, 11(85):112, 1945.
- [28] L. Issler. *Festigkeitsverhalten metallischer Werkstoffe bei mehrachsiger phasenverschobener Schwingbeanspruchung*. PhD thesis, Staatl. Materialprüfungsanst. TU Stuttgart, 1973.
- [29] E. El-Magd and S. Mielke. Dauerfestigkeit bei überlagerter zweiachsiger statischer beanspruchung. *Konstruktion*, 29(7):253–257, 1977.
- [30] A. Troost, E. El-Magd, and S. Keil. Grundlagen zur berechnung der schwingfestigkeit bei mehrachsiger beanspruchung ohne phasenverschiebung: Schwingfestigkeit ohne phasenverschiebung. *Forschungsbericht des Landes NRW, Fachgruppe Maschinenbau/verfahrenstechnik, Westd. Verlag*, Nr 2812, 1979.
- [31] F. J. Baier. *Zeit-und Dauerfestigkeit bei überlagerter statischer und schwingender Zug-, Druck-und Torsionsbeanspruchung*. PhD thesis, Diss. Staatl. Materialprüfungsanst. TU Stuttgart, 1970.
- [32] A. Galtier. *Contribution à l'étude de l'endommagement des aciers sous sollicitations uni ou multiaxiales*. PhD thesis, ENSAM CER de Bordeaux, France, 1993.
- [33] R. Heidenreich. Schubspannungsintensitätshypothese - dauerschwingfestigkeit bei mehrachsiger beanspruchung. *Forschungshefte FKM*, Heft 105, 1983.
- [34] R. Heidenreich and H. Zenner. Schubspannungsintensitaetshypotheseerweiterung und experimentelle abschaetzung einer neuen festigkeitshypothese fuer schwingende beanspruchung. *Forschungshefte FKM*, (77), 1979.
- [35] H. Zenner and R. Heidenreich. Festigkeitshypothese - berechnung der dauerfestigkeit für beliebige beanspruchungskombinationen. *Forschungshefte FKM*, Heft 55, 1979.
- [36] C. Froustey, S. Lasserre, and L. Dubar. Validité des critères de fatigue multiaxiale à l'endurance en flexion-torsion. *Mat-Tech*, 92:79–82, 1992.
- [37] S. Mielke. *Festigkeitsverhalten metallischer Werkstoffe unter zweiachsig schwingender Beanspruchung mit verschiedenen Spannungszeitverläufen*. PhD thesis, Aachen, Techn. Hochsch., Fak. für Maschinenwesen,, 1980.

Bibliography

- [38] W. Lempp. *Festigkeitsverhalten von Stählen bei mehrachsiger Dauerschwingbeanspruchung durch Normalspannungen mit überlagerten phasengleichen und phasenverschobenen Schubspannungen*. PhD thesis, Staatl. Materialprüfungsanst., 1977.
- [39] F. Klubberg. *Zweiachsige Schwingfestigkeitsversuche mit drei schwingenden Lastkomponenten und vergleichende Auswertung nach verschiedenen statistischen Methoden*. PhD thesis, RWTH Aachen, 1985.
- [40] A. Troost, O. Akin, and F. Klubberg. Dauerfestigkeitsverhalten metallischer Werkstoffe bei zweiachsiger Beanspruchung durch drei phasenverschoben schwingende Lastspannungen. *Konstruktion*, 39:479–488, 1987.
- [41] P. Grün, A. Troost, O. Akin, and F. Klubberg. Langzeit- und dauerschwingfestigkeit des vergütungsstahls 25crmo4 bei mehrachsiger Beanspruchung durch drei schwingende Lastspannungen. *Materialwissenschaft und Werkstofftechnik*, 22(3):73–80, 1991.
- [42] T. Palin-Luc. *Fatigue multiaxiale d'une fonte GS sous sollicitations combinées d'amplitude variable*. PhD thesis, ENSAM CER de Bordeaux, 1996.
- [43] M. Bennebach. *Fatigue multiaxiale d'une fonte GS. Influence de l'entaille et d'un traitement de surface*. PhD thesis, ENSAM CER de Bordeaux, 1993.
- [44] L. Susmel. *La progettazione a fatica in presenza di stati complessi di sollecitazione*. PhD thesis, Università degli Studi di Padova, 2002.

List of Figures

2.1.1.3D-coordinate system.	6
2.1.2.Element showing stress components for plane stress, $\sigma_z = 0$	8
2.2.1.Failure locus showing the fatigue limits for fully reversed stresses in shear and normal stress.	9
2.2.2.Haigh-diagram.	10
4.8.1.Example of a failure assessment diagram for the Tresca-Sines criterion.	27
4.10.Cyclic stresses for dynamically loaded mechanical component.	31
5.2.1.Failure assessment diagram, $R = -1$ and $\alpha_{ij} = 0^\circ$. Test data are 34 fatigue tests for carbon/low alloy steels.	35
5.2.2.Failure assessment diagram, $R = -1$ and $\alpha_{ij} = 0^\circ$. Test data are 13 fatigue tests for 76S-T61.	36
5.2.3.Failure assessment diagram, $R = -1$ and $\alpha_{ij} = 0^\circ$. Test data are 12 fatigue tests for cast irons.	36
5.3.1.Predictions and their distribution for the criteria normal stress, Mises-Sines and Tresca-Sines for all 268 tests.	38
5.3.2.Histograms of all predictions from the ASME criterion and Findley $k(\sigma_A)$ and $k(\tau_W)$ for 268 tests.	39
5.4.1.Stresses throughout the cycle on critical planes predicted by the critical-plane criteria.	46
6.3.1.Stress cycle with one shear and one normal stress component.	51

List of Tables

2.1.	Support factors for types of material groups according to FKM-Richtlinie.	16
3.1.	Given and calculated material parameters for carbon steels and alloyed steels.	18
3.2.	Given and calculated material parameters for aluminium alloys and cast irons.	19
4.1.	List of materials collected from the literature and their references. For some materials, several data sets exist and each individual data set is numbered with a number inside a parenthesis.	30
4.2.	Extreme values of stresses during a cycle of a dynamically loaded component.	32
4.3.	Material parameters for a constructed steel according to FKM-Richtlinie and assumed to be valid for the stress cycle given in figure (4.10.1).	32
5.1.	Average values of M , $k(\sigma_A)$ and $k(\tau_W)$ reported in table 3.1 and 3.2 with respect to material grouping. Only values used in the fatigue analysis was counted in.	33
5.2.	Comparison of predictions for all criteria and different loading cases. The predictions are presented as the mean value plus/minus one standard deviation, $m_p \pm s_p$	41
5.3.	Comparison of predictions for all criteria, a selection of stress components present, and different groups of materials. No selection of stress-ratios or the like have been made. The predictions are presented as the mean value plus/minus one standard deviation, $m_p \pm s_p$	42
5.4.	Results of stress-cycle assessment for all criteria and both assessment methods normalized with σ_W	44
5.5.	Results of stress-cycle assessment for all criteria and both assessment methods. The names for the criteria are shortened, so that NS corresponds to the normal stress criterion etc.	45

List of Tables

A.1. Specimens, number of cycles the fatigue limits given in table 3.1 and 3.2 are valid for, and their method of determination.	68
A.2. Data collected from Gough [25]. Material parameters given in table 3.1.	69
A.3. Data collected from Gough [25]. Material parameters given in table 3.1 and 3.2.	70
A.4. Data collected from Froustey [24, 21]. Material parameters given in table 3.1.	71
A.5. Data collected from Carpinteri [3]. Material parameters given in table 3.1 and 3.2.	72
A.6. Data collected from Zenner [22]. Material parameters given in table 3.1.	73
A.7. Data from collected from Zenner [22]. Material parameters given in table 3.1.	74
A.8. Data collected from Troost [6]. Material parameters given in table 3.1.	75
A.9. Data collected from Troost [6]. Material parameters given in table 3.1 and 3.2.	76
A.10. Data from Findley [26]. Material parameters given in table 3.1.	77
A.11. Data collected from Banvillet [23]. Material parameters given in table 3.1 and 3.2.	78
B.1. Predictions for all tests and selected criteria.	80
B.2. Predictions for all tests and selected criteria.	81
B.3. Predictions for all tests and selected criteria.	82
B.4. Predictions for all tests and selected criteria.	83
B.5. Predictions for all tests and selected criteria.	84
B.6. Predictions for all tests and selected criteria.	85
B.7. Predictions for all tests and selected criteria.	86

A. Material Data

A. Material Data

Table A.1.: Specimens, number of cycles the fatigue limits given in table 3.1 and 3.2 are valid for, and their method of determination.

Material	Ref.	Spec.	N_f	Determined by
<i>Carbon and low alloy steels</i>				
0.1 % C Steel	[25]	SS	10^7	S-N testing
XC18 Steel	[21]	-	10^6	Staircase method, 10-12 spec.
Mild Steel	[3]	SS	10^6 or more	-
St35 Steel	[22]	HS	$2 \cdot 10^6$	-
St60 Steel	[6]	HS	$2 \cdot 10^6$	-
Swedish Hard Steel	[3]	SS	10^6 or more	-
Ck 35 V	[6]	HS	10^7	-
C20 annealed Steel	[23]	SS	10^6 or more	Staircase method, ≥ 15 spec.
34Cr4 (1)	[22]	HS	$1,5 \cdot 10^6$	Staircase method
34Cr4 (2)	[22]	SS	$2 \cdot 10^6$	Staircase method
34Cr4 (3)	[22]	SS	$1,5 \cdot 10^6$	Staircase method
30CrMo16 (1)	[24, 21]	SS	10^6	S-N testing
30CrMo16 (2)	[23]	SS	10^6 or more	Staircase method, ≥ 15 spec.
25CrMo4 (1)	[21]	HS	$2 \cdot 10^6$	Staircase method, ≥ 15 spec.
25CrMo4 (2)	[22]	HS	-	Staircase method.
S65A	[25]	SS	10^7	S-N testing
42CrMo4	[22]	HS	$2 \cdot 10^6$	-
25CrMo4 (3)	[6]	HS	10^7	-
3.5% NiCr steel	[25]	SS	10^7	S-N testing
34CrMo4 V	[6]	SS	10^7	-
<i>Aluminium</i>				
76S-T61 (1)	[26]	SS	10^6	S-N testing
76S-T61 (2)	[26]	SS	10^7	S-N testing
76S-T61 (3)	[26]	SS	10^8	S-N testing
<i>Nodular graphite cast irons</i>				
“Sial” cast iron	[20]	SS	10^7	S-N testing
EN-GJS800-2	[23]	-	10^6 or more	Staircase method, ≥ 15 spec.
<i>Lamellar graphite cast irons</i>				
GG30	[6]	SS	10^7	-
Cast iron	[3]	SS	-	-

() Stress values are calculated for comparability but not used in later calculations.
 SS = Solid specimen, HS = Hollow specimen, - = No Info

Table A.2.: Data collected from Gough [25]. Material parameters given in table 3.1.

Nr.	σ_{xa} (MPa)	σ_{xm} (MPa)	σ_{ya} (MPa)	σ_{ym} (MPa)	τ_{xya} (MPa)	τ_{xym} (MPa)	α_y ($^\circ$)	α_{xy} ($^\circ$)
0.1% C Steel from Gough [25].								
1	268.7	0	0	0	0	0	0	0
2	262.5	0	0	0	35.5	0	0	0
3	242.4	0	0	0	69.5	0	0	0
4	205.4	0	0	0	103.4	0	0	0
5	146.7	0	0	0	126.6	0	0	0
6	78.7	0	0	0	146.7	0	0	0
7	0	0	0	0	151.3	0	0	0
S65A from Gough [25].								
152	552.9	266.4	0	0	0	0	0	0
153	532.8	532.8	0	0	0	0	0	0
154	0	0	0	0	339	169.9	0	0
155	0	0	0	0	343.6	343.6	0	0
156	549.8	0	0	0	0	169.9	0	0
157	540.5	0	0	0	0	343.6	0	0
158	556	266.4	0	0	0	169.9	0	0
159	556	266.4	0	0	0	343.6	0	0
160	469.5	532.8	0	0	0	169.9	0	0
161	472.6	532.8	0	0	0	343.6	0	0
162	0	266.4	0	0	312	0	0	0
163	0	532.8	0	0	284.2	0	0	0
164	0	266.4	0	0	304.3	169.9	0	0
165	0	532.8	0	0	281.1	169.9	0	0
166	0	266.4	0	0	308.9	343.6	0	0
167	0	532.8	0	0	293.4	343.6	0	0
168	547.5	0	0	0	156	0	0	0
169	389.2	0	0	0	259.5	0	0	0
170	168.3	0	0	0	335.9	0	0	0
171	496.5	266.4	0	0	141.3	169.9	0	0
172	374.5	266.4	0	0	249.4	169.9	0	0
173	161.4	266.4	0	0	322	169.9	0	0
174	428.6	532.8	0	0	121.2	343.6	0	0
175	315.1	532.8	0	0	210	343.6	0	0
176	126.6	532.8	0	0	251.7	343.6	0	0
177	386.1	266.4	0	0	257.1	0	0	0
178	383.8	0	0	0	255.6	169.9	0	0

A. Material Data

Table A.3.: Data collected from Gough [25]. Material parameters given in table 3.1 and 3.2.

Nr.	σ_{xa} (MPa)	σ_{xm} (MPa)	σ_{ya} (MPa)	σ_{ym} (MPa)	τ_{xya} (MPa)	τ_{xym} (MPa)	α_y ($^\circ$)	α_{xy} ($^\circ$)
3.5% NiCr Steel from Gough [25].								
200	540.4	0	0	0	0.0	0	0	0
201	538.9	0	0	0	71.0	0	0	0
202	491.0	0	0	0	142.0	0	0	0
203	410.7	0	0	0	205.4	0	0	0
204	328.9	0	0	0	284.1	0	0	0
205	179.1	0	0	0	333.5	0	0	0
206	0.0	0	0	0	352.0	0	0	0
"Silal" Cast Iron from Gough [25].								
243	240.9	0	0	0	0.0	0	0	0
244	234.7	0	0	0	30.9	0	0	0
245	210.0	0	0	0	60.2	0	0	0
246	194.5	0	0	0	97.3	0	0	0
247	152.9	0	0	0	132.8	0	0	0
248	89.6	0	0	0	166.8	0	0	0
249	0.0	0	0	0	219.2	0	0	0

Table A.4.: Data collected from Froustey [24, 21]. Material parameters given in table 3.1.

Nr.	σ_{xa} (MPa)	σ_{xm} (MPa)	σ_{ya} (MPa)	σ_{ym} (MPa)	τ_{xya} (MPa)	τ_{xym} (MPa)	α_y ($^\circ$)	α_{xy} ($^\circ$)
XC18 Steel from Froustey/Lasserre [21].								
8	310	0	0	0	0	0	0	0
9	0	0	0	0	179	0	0	0
10	230	0	0	0	133	0	0	0
11	230	0	0	0	133	0	0	45
12	242	0	0	0	140	0	0	90
30CrMo16 (1) from Froustey/Lasserre [24, 21].								
95	630	300	0	0	0	0	0	0
96	0	300	0	0	370	0	0	0
97	211	300	0	0	365	0	0	0
98	220	300	0	0	385	0	0	90
99	590	300	0	0	148	0	0	0
100	563	300	0	0	141	0	0	45
101	540	300	0	0	135	0	0	90
102	480	300	0	0	277	0	0	0
103	480	300	0	0	277	0	0	45
104	470	300	0	0	271	0	0	60
105	473	300	0	0	273	0	0	90
106	710	0	0	0	0	0	0	0
107	0	0	0	0	450	0	0	0
108	485	0	0	0	280	0	0	0
109	480	0	0	0	277	0	0	90
110	0	300	0	0	395	0	0	0
25CrMo4 (1) from Mielke [37].								
140	361	0	0	0	0	0	0	0
141	270	0	0	0	135	0	0	0
142	261	0	0	0	131	0	0	60
143	277	0	0	0	139	0	0	90

A. Material Data

Table A.5.: Data collected from Carpinteri [3]. Material parameters given in table 3.1 and 3.2.

Nr.	σ_{xa} (MPa)	σ_{xm} (MPa)	σ_{ya} (MPa)	σ_{ym} (MPa)	τ_{xya} (MPa)	τ_{xym} (MPa)	α_y ($^\circ$)	α_{xy} ($^\circ$)
Mild steel from Nishihara/Kawamoto [27].								
13	245.3	0	0	0	0	0	0	0
14	235.6	0	0	0	48.9	0	0	0
15	187.3	0	0	0	93.6	0	0	0
16	101.3	0	0	0	122.3	0	0	0
17	0	0	0	0	142.3	0	0	0
18	194.2	0	0	0	97.1	0	0	60
19	108.9	0	0	0	131.5	0	0	60
20	235.6	0	0	0	48.9	0	0	90
21	208.1	0	0	0	104.1	0	0	90
22	112.6	0	0	0	136	0	0	90
Swedish hard steel from Nishihara/Kawamoto [27].								
42	327.7	0	0	0	0	0	0	0
43	308	0	0	0	63.9	0	0	0
44	255.1	0	0	0	127.5	0	0	0
45	141.9	0	0	0	171.3	0	0	0
46	0	0	0	0	201.1	0	0	0
47	255.1	0	0	0	127.5	0	0	30
48	142	0	0	0	171.2	0	0	30
49	255.1	0	0	0	127.5	0	0	60
50	147.2	0	0	0	177.6	0	0	60
51	308	0	0	0	63.9	0	0	90
52	264.9	0	0	0	132.4	0	0	90
53	152.5	0	0	0	184.2	0	0	90
Grey Cast Iron from Nishihara/Kawamoto [27].								
261	93.2	0	0	0	0	0	0	0
262	95.2	0	0	0	19.7	0	0	0
263	83.4	0	0	0	41.6	0	0	0
264	56.3	0	0	0	68	0	0	0
265	0	0	0	0	94.2	0	0	0
266	104.2	0	0	0	21.6	0	0	90
267	97.1	0	0	0	48.6	0	0	90
268	71.3	0	0	0	86.1	0	0	90

Table A.6.: Data collected from Zenner [22]. Material parameters given in table 3.1.

Nr.	σ_{xa} (MPa)	σ_{xm} (MPa)	σ_{ya} (MPa)	σ_{ym} (MPa)	τ_{xya} (MPa)	τ_{xym} (MPa)	α_y ($^\circ$)	α_{xy} ($^\circ$)
St35 Steel from Issler [28].								
23	139	153	139	153	0	0	0	0
24	147	162	147	162	0	0	60	0
25	129	142	129	142	0	0	90	0
26	110	121	110	121	0	0	120	0
27	100	110	100	110	0	0	180	0
28	154	169	77	92	0	0	0	0
29	149	164	75	89	0	0	60	0
30	142	156	11	85	0	0	90	0
31	123	135	62	74	0	0	180	0
32	157	173	79	0	0	0	0	0
33	145	160	73	0	0	0	90	0
34	118	130	59	0	0	0	180	0
25CrMo4 (2) from Mielke [37].								
144	261	170	261	340	0	0	0	0
145	275	170	275	340	0	0	60	0
146	240	170	240	340	0	0	90	0
147	196	170	196	340	0	0	180	0
148	0	170	220	340	110	0	0	60
149	0	170	233	340	117	0	0	90
150	0	170	155	340	155	0	0	60
151	0	170	159	340	159	0	0	90
42CrMo4 from Lempp [38].								
179	328	0	0	0	157	0	0	0
180	286	0	0	0	137	0	0	90
181	233	0	0	0	224	0	0	0
182	213	0	0	0	205	0	0	90
183	280	280	0	0	134	0	0	0
184	271	271	0	0	130	0	0	90
185	266	0	0	0	128	128	0	0
186	283	0	0	0	136	136	0	90
187	333	0	0	0	160	160	0	180

A. Material Data

Table A.7.: Data from collected from Zenner [22]. Material parameters given in table 3.1.

Nr.	σ_{xa} (MPa)	σ_{xm} (MPa)	σ_{ya} (MPa)	σ_{ym} (MPa)	τ_{xya} (MPa)	τ_{xym} (MPa)	α_y (°)	α_{xy} (°)
34Cr4 (1) from Heidenreich [33, 34, 35].								
68	225	275	225	275	0	0	0	0
69	225	275	225	275	0	0	60	0
70	190	232	190	232	0	0	180	0
71	205	250	205	250	96	0	0	0
72	175	214	175	214	82	0	180	0
73	181	221	181	221	85	85	0	0
74	195	238	195	238	92	92	0	90
75	192	234	192	234	90	90	60	90
76	180	220	180	220	85	85	180	90
34Cr4 (2) from Heidenreich [34, 35].								
77	314	0	0	0	157	0	0	0
78	315	0	0	0	158	0	0	60
79	316	0	0	0	158	0	0	90
80	315	0	0	0	158	0	0	120
81	224	0	0	0	224	0	0	90
82	380	0	0	0	95	0	0	90
83	316	0	0	0	158	158	0	0
84	314	0	0	0	157	157	0	60
85	315	0	0	0	158	158	0	90
86	279	279	0	0	140	0	0	0
87	284	284	0	0	142	0	0	90
88	355	0	0	0	89	178	0	0
89	212	212	0	0	212	0	0	90
90	129	0	0	0	258	0	0	90
34Cr4 (3) from Heidenreich [34, 35].								
91	280	0	0	0	140	280	0	0
92	309	0	0	0	155	309	0	180
93	320	-160	0	0	160	160	0	0
94	350	-175	0	0	175	175	0	180

Table A.8.: Data collected from Troost [6]. Material parameters given in table 3.1.

Nr.	σ_{xa} (MPa)	σ_{xm} (MPa)	σ_{ya} (MPa)	σ_{ym} (MPa)	τ_{xya} (MPa)	τ_{xym} (MPa)	α_y ($^\circ$)	α_{xy} ($^\circ$)
St60 Steel from El Magd/Troost [29],[30].								
35	290.4	0	0	306.8	0	0	0	0
36	259	0	0	460.2	0	0	0	0
37	286.5	76.7	0	306.8	0	0	0	0
38	259	76.7	0	460.2	0	0	0	0
39	280.6	153.4	0	153.4	0	0	0	0
40	278.6	153.4	0	306.8	0	0	0	0
41	262.9	153.4	0	460.2	0	0	0	0
Ck35 V Steel from Baier [31].								
54	273	0	0	0	0	156.5	0	0
55	273	0	0	0	0	303.61	0	0
56	216	0	0	0	0	441.33	0	0
57	229	229	0	0	0	172.15	0	0
58	181	181	0	0	0	344.3	0	0
59	0	0	0	0	191	191	0	0
60	0	-547.75	0	0	239	0	0	0
61	0	-275.44	0	0	229	0	0	0
62	0	294.22	0	0	176	0	0	0
63	0	441.33	0	0	141	0	0	0
64	0	588.44	0	0	130	0	0	0
25CrMo4 (3) from Klubberg/Troost/Grün [39],[40],[41].								
188	205	340	205.0	221	102.5	0	0	90
189	185	340	185.0	221	92.5	0	0	90
190	218.8	255	164.1	210.8	109.4	0	0	0
191	207.5	255	155.6	210.8	103.75	0	0	90
192	212.1	255	159.1	210.8	106.05	0	0	180
193	225	255	168.8	210.8	112.5	0	0	90
194	222.1	255	166.6	210.8	111.05	0	0	45
195	205	255	153.8	210.8	102.5	0	0	90
196	215	255	161.3	210.8	107.5	0	0	135
197	187.9	255	140.9	210.8	93.95	0	0	0
198	223.6	255	167.7	210.8	111.8	0	0	90
199	215	255	161.3	210.8	107.5	88.4	0	135

A. Material Data

Table A.9.: Data collected from Troost [6]. Material parameters given in table 3.1 and 3.2.

Nr.	σ_{xa} (MPa)	σ_{xm} (MPa)	σ_{ya} (MPa)	σ_{ym} (MPa)	τ_{xya} (MPa)	τ_{xym} (MPa)	α_y ($^\circ$)	α_{xy} ($^\circ$)
34CrMo4 V from Baier [31].								
207	378	0	0	0	0	107.0	0	0
208	353	0	0	0	0	217.7	0	0
209	329	0	0	0	0	324.7	0	0
210	320	0	0	0	0	431.7	0	0
211	294	294	0	0	0	645.6	0	0
212	88	88	0	0	0	794.6	0	0
213	311	311	0	0	0	194.8	0	0
214	273	0	0	0	0	489.0	0	0
215	0	0	0	0	256	256	0	0
216	0	-550.1	0	0	343	0	0	0
217	0	-179.5	0	0	284	0	0	0
218	0	179.5	0	0	283	0	0	0
219	0	351.4	0	0	235	0	0	0
220	0	511.9	0	0	222	0	0	0
221	0	695.2	0	0	156	0	0	0
GG30 from Baier [31].								
254	145	0	0	0	0	74	0	0
255	127	0	0	0	0	112.5	0	0
256	107	0	0	0	0	146.5	0	0
257	99	0	0	0	0	186.5	0	0
258	96.5	0	0	0	0	108.0	0	0
259	75	0	0	0	0	217.6	0	0
260	53.5	0	0	0	0	196.8	0	0

Table A.10.: Data from Findley [26]. Material parameters given in table 3.1.

Nr.	σ_{xa} (MPa)	σ_{xm} (MPa)	σ_{ya} (MPa)	σ_{ym} (MPa)	τ_{xya} (MPa)	τ_{xym} (MPa)	α_y ($^\circ$)	α_{xy} ($^\circ$)
76S-T61 (1) for 10^6 cycles.								
222	217.9	0.0	0	0	0.0	0	0	0
223	0.0	0.0	0	0	143.4	0	0	0
224	215.8	0.0	0	0	44.7	0.0	0	0
225	171.0	0.0	0	0	85.5	0.0	0	0
226	153.1	82.7	0	0	76.5	41.4	0	0
227	129.6	206.8	0	0	64.8	103.4	0	0
228	139.3	0.0	0	0	101.9	0.0	0	0
229	104.5	0.0	0	0	126.2	0.0	0	0
76S-T61 (2) for 10^7 cycles.								
230	188.2	0.0	0	0	0.0	0.0	0	0
231	0.0	0.0	0	0	119.3	0	0	0
232	180.6	0.0	0	0	37.4	0.0	0	0
233	139.3	0.0	0	0	69.6	0.0	0	0
234	136.5	82.7	0	0	68.3	41.4	0	0
235	122.0	206.8	0	0	61.0	103.4	0	0
236	117.9	0.0	0	0	86.2	0.0	0	0
237	86.7	0.0	0	0	104.1	0.0	0	0
76S-T61 (3) for 10^8 cycles.								
238	170.3	0.0	0	0	0.0	0.0	0	0
239	0.0	0.0	0	0	109.6	0	0	0
240	124.8	0.0	0	0	62.4	0.0	0	0
241	12.4	82.7	0	0	62.1	41.4	0	0
242	102.7	0.0	0	0	75.2	0.0	0	0

A. Material Data

Table A.11.: Data collected from Banvillet [23]. Material parameters given in table 3.1 and 3.2.

Nr.	σ_{xa} (MPa)	σ_{xm} (MPa)	σ_{ya} (MPa)	σ_{ym} (MPa)	τ_{xya} (MPa)	τ_{xym} (MPa)	α_y ($^\circ$)	α_{xy} ($^\circ$)
C20 annealed Steel from Galtier [32].								
65	246	0	0	0	138	0	0	0
66	246	0	0	0	138	0	0	45
67	264	0	0	0	148	0	0	90
30CrMo16 (2) from Froustey [36].								
111	575	375	0	0	0	0	0	0
112	558	428	0	0	0	0	0	0
113	627	273	0	0	0	0	0	0
114	679	156	0	0	0	0	0	0
115	519	0	0	0	291	0	0	0
116	514	0	0	0	288	0	0	90
117	451	294	0	0	250	191	0	0
118	462	294	0	0	258	191	0	90
119	474	294	0	0	265	0	0	45
120	464	294	0	0	259	0	0	60
121	554	287	0	0	135	0	0	45
122	474	0	0	0	265	0	0	90
123	220	199	0	0	368	0	0	90
124	470	299	0	0	261	0	0	90
125	527	287	0	0	129	0	0	90
126	433	472	0	0	240	0	0	90
127	418	622	0	0	234	0	0	90
128	0	299	0	0	396	0	0	0
129	0	486	0	0	411	0	0	0
130	0	655	0	0	364	0	0	0
131	482	0	0	0	268	0	0	0
132	207	299	0	0	350	0	0	0
133	474	294	0	0	265	0	0	0
134	584	281	0	0	142	0	0	0
135	447	473	0	0	252	0	0	0
136	425	635	0	0	223	0	0	0
137	235	745	0	0	0	0	0	0
138	251	704	0	0	0	0	0	0
139	527	222	0	0	0	0	0	0
EN-GJS800-2 Cast Iron from [42],[43].								
250	228	0	0	0	132	0	0	0
251	245	0	0	0	142	0	0	90
252	199	0	0	0	147	0	0	0
253	184	225	0	0	0	0	0	0

B. Predictions

B. Predictions

Table B.1.: Predictions for all tests and selected criteria.

Nr.	Normal stress	σ_{ar}/σ_W	
		Findley (τ_W)	Findley (τ_W)-ASME
1	1.02	1.02	1.02
2	1.02	1.03	1.03
3	0.99	1.05	1.05
4	0.95	1.07	1.07
5	0.84	1.05	1.05
6	0.73	1.05	1.05
7	0.58	1.02	1.02
8	1.00	1.00	1.00
9	0.58	1.00	1.00
10	0.94	1.08	1.08
11	0.87	1.04	1.00
12	0.78	0.98	0.83
13	1.04	1.04	1.04
14	1.04	1.07	1.07
15	0.96	1.08	1.08
16	0.78	1.03	1.03
17	0.60	1.04	1.04
18	0.89	1.04	0.98
19	0.73	1.09	1.03
20	1.00	1.01	1.00
21	0.88	1.00	0.89
22	0.63	1.11	1.00
23	0.84	0.46	0.46
24	0.89	1.04	0.91
25	0.78	1.10	0.99
26	0.66	1.04	0.97
27	0.60	0.99	0.99
28	0.93	0.72	0.72
29	0.90	0.89	0.86
30	0.86	0.89	0.89
31	0.74	0.98	0.98
32	0.95	0.69	0.69
33	0.88	0.94	0.91
34	0.71	0.90	0.90
35	0.98	1.16	1.16
36	0.88	1.17	1.17
37	1.00	1.20	1.20
38	0.91	1.21	1.21
39	1.01	1.15	1.15
40	1.01	1.22	1.22
41	0.95	1.27	1.27
42	1.04	1.04	1.04

Table B.2.: Predictions for all tests and selected criteria.

Nr.	Normal stress	σ_{ar}/σ_W	
		Findley (τ_W)	Findley (τ_W)-ASME
43	1.02	1.05	1.05
44	0.98	1.08	1.08
45	0.82	1.04	1.04
46	0.64	1.02	1.02
47	0.95	1.07	1.05
48	0.79	1.03	1.01
49	0.88	1.03	0.96
50	0.74	1.07	0.99
51	0.98	1.00	0.98
52	0.84	0.99	0.86
53	0.64	1.10	0.96
54	0.89	1.12	0.66
55	0.95	1.37	0.90
56	0.87	1.42	1.05
57	0.96	1.27	0.87
58	0.85	1.33	0.98
59	0.78	1.06	1.06
60	0.56	1.10	1.10
61	0.62	1.06	1.06
62	0.71	1.31	1.31
63	0.69	1.39	1.39
64	0.75	1.59	1.59
65	0.93	1.07	1.07
66	0.87	1.02	0.99
67	0.80	0.96	0.83
68	0.89	0.46	0.46
69	0.89	0.98	0.86
70	0.75	1.15	1.15
71	1.09	0.89	0.89
72	0.75	1.15	1.15
73	1.04	0.81	0.81
74	0.91	0.85	0.76
75	0.96	1.08	0.99
76	0.72	1.23	1.17
77	0.92	1.02	1.02
78	0.83	0.97	0.91
79	0.77	0.90	0.79
80	0.83	0.97	0.89
81	0.63	1.07	0.91
82	0.93	0.95	0.93
83	1.01	1.16	0.96
84	0.90	1.04	0.84

B. Predictions

Table B.3.: Predictions for all tests and selected criteria.

Nr.	Normal stress	σ_{ar}/σ_w	
		Findley (τ_w)	Findley (τ_w)-ASME
85	0.80	0.99	0.74
86	0.99	1.16	1.16
87	0.89	1.09	0.95
88	0.98	1.12	0.83
89	0.70	1.21	1.06
90	0.65	1.10	1.02
91	0.97	1.14	0.80
92	0.77	1.18	0.96
93	0.93	1.12	0.81
94	0.82	1.07	0.95
95	1.09	1.07	1.07
96	0.63	1.08	1.08
97	0.83	1.17	1.17
98	0.69	1.22	1.13
99	1.08	1.13	1.13
100	1.02	1.06	1.05
101	0.96	0.96	0.94
102	1.04	1.20	1.20
103	0.98	1.18	1.13
104	0.92	1.14	1.06
105	0.86	1.10	0.93
106	1.08	1.08	1.08
107	0.68	1.10	1.10
108	0.93	1.05	1.05
109	0.73	0.94	0.77
110	0.67	1.14	1.14
111	1.01	0.97	0.97
112	1.01	0.97	0.97
113	1.04	1.01	1.01
114	1.06	1.04	1.04
115	0.94	1.06	1.06
116	0.74	0.94	0.78
117	0.99	1.05	1.03
118	0.82	1.03	0.85
119	0.92	1.09	1.06
120	0.87	1.05	0.99
121	0.96	0.99	0.98
122	0.69	0.87	0.72
123	0.61	1.07	0.98
124	0.82	1.02	0.87
125	0.90	0.89	0.87
126	0.85	1.05	0.91

Table B.4.: Predictions for all tests and selected criteria.

Nr.	Normal stress	σ_{ar}/σ_w	
		Findley (τ_w)	Findley (τ_w)-ASME
127	0.89	1.12	0.97
128	0.65	1.09	1.09
129	0.72	1.23	1.23
130	0.70	1.21	1.21
131	0.87	0.98	0.98
132	0.77	1.08	1.08
133	0.97	1.12	1.12
134	1.02	1.05	1.05
135	1.00	1.17	1.17
136	1.01	1.18	1.18
137	0.85	0.81	0.81
138	0.85	0.81	0.81
139	1.07	1.04	1.04
140	1.00	1.00	1.00
141	0.90	0.99	0.99
142	0.78	0.91	0.85
143	0.77	0.91	0.79
144	0.91	0.69	0.69
145	0.95	1.16	1.03
146	0.86	1.22	1.11
147	0.73	1.18	1.18
148	0.84	1.15	0.97
149	0.84	1.16	1.03
150	0.77	1.23	1.05
151	0.67	1.25	1.12
152	1.06	1.08	1.08
153	1.14	1.18	1.18
154	0.65	0.96	0.96
155	0.74	1.02	1.02
156	0.95	1.06	0.82
157	0.95	1.17	0.78
158	1.07	1.20	0.97
159	1.09	1.32	0.87
160	1.04	1.18	0.97
161	1.06	1.30	0.89
162	0.59	1.03	1.03
163	0.61	1.15	1.15
164	0.65	1.05	1.05
165	0.68	1.17	1.17
166	0.74	1.11	1.11
167	0.77	1.26	1.26
168	1.01	1.05	1.05

B. Predictions

Table B.5.: Predictions for all tests and selected criteria.

Nr.	Normal stress	σ_{ar}/σ_w	
		Findley (τ_w)	Findley (τ_w)-ASME
169	0.89	1.02	1.02
170	0.74	1.00	1.00
171	1.06	1.15	1.05
172	1.00	1.13	1.13
173	0.85	1.16	1.16
174	1.08	1.25	1.05
175	1.02	1.16	1.16
176	0.84	1.17	1.17
177	0.97	1.20	1.20
178	0.94	1.10	0.96
179	0.98	1.07	1.07
180	0.72	0.84	0.74
181	0.93	1.11	1.11
182	0.60	1.00	0.84
183	1.01	1.22	1.22
184	0.87	1.11	0.98
185	0.87	1.00	0.81
186	0.73	0.94	0.68
187	0.93	1.19	0.92
188	0.85	1.38	1.25
189	0.68	1.34	1.28
190	0.99	1.16	1.16
191	0.73	1.12	0.98
192	0.96	1.14	1.08
193	0.80	1.29	1.13
194	0.86	1.29	1.14
195	0.71	1.28	1.10
196	0.81	1.30	1.17
197	0.72	1.24	1.24
198	0.76	1.35	1.27
199	0.79	1.40	1.24
200	1.00	1.00	1.00
201	1.01	1.02	1.02
202	0.98	1.02	1.02
203	0.92	1.00	1.00
204	0.91	1.07	1.07
205	0.80	1.06	1.06
206	0.65	1.00	1.00
207	0.99	1.15	0.84
208	0.94	1.27	0.78
209	0.90	1.38	0.90
210	0.91	1.53	1.06

Table B.6.: Predictions for all tests and selected criteria.

Nr.	Normal stress	σ_{ar}/σ_w	
		Findley (τ_w)	Findley (τ_w)-ASME
211	1.08	2.14	1.71
212	0.64	1.65	1.52
213	1.01	1.50	1.16
214	0.82	1.51	1.10
215	0.82	1.18	1.18
216	0.75	1.17	1.17
217	0.69	0.98	0.98
218	0.80	1.29	1.29
219	0.73	1.40	1.40
220	0.75	1.62	1.62
221	0.67	1.70	1.70
222	1.00	1.00	1.00
223	0.66	1.00	1.00
224	1.03	1.05	1.05
225	0.95	1.03	1.03
226	1.06	1.06	1.06
227	1.24	1.17	1.17
228	0.89	1.01	1.01
229	0.87	1.07	1.07
230	1.00	1.00	1.00
231	0.63	1.00	1.00
232	1.00	1.02	1.02
233	0.89	0.98	0.98
234	1.11	1.10	1.10
235	1.36	1.24	1.24
236	0.87	1.01	1.01
237	0.83	1.04	1.04
238	1.00	1.00	1.00
239	0.64	1.00	1.00
240	0.88	0.97	0.97
241	0.61	0.83	0.83
242	0.84	0.96	0.96
243	1.05	1.05	1.05
244	1.04	1.04	1.04
245	0.98	0.99	0.99
246	1.02	1.05	1.05
247	1.00	1.05	1.05
248	0.94	1.03	1.03
249	0.95	1.10	1.10
250	0.98	1.05	1.05
251	0.83	1.11	0.91
252	0.94	1.03	1.03

B. Predictions

Table B.7.: Predictions for all tests and selected criteria.

Nr.	Normal stress	$\sigma_{\text{ar}}/\sigma_{\text{W}}$	
		Findley (τ_{W})	Findley (τ_{W})-ASME
253	0.90	1.05	1.05
254	1.03	1.32	1.07
255	0.97	1.42	1.18
256	0.93	1.49	1.28
257	0.99	1.68	1.48
258	0.79	1.21	1.02
259	0.95	1.73	1.58
260	0.80	1.49	1.38
261	0.97	0.97	0.97
262	1.03	1.03	1.03
263	1.05	1.06	1.06
264	1.06	1.08	1.08
265	0.98	1.03	1.03
266	1.08	1.13	1.10
267	1.01	1.19	1.09
268	0.98	1.17	1.08
<hr/>			
max	1.36	2.14	1.71
min	0.56	0.46	0.46
m_p	0.88	1.10	1.03
s_p	0.14	0.18	0.17